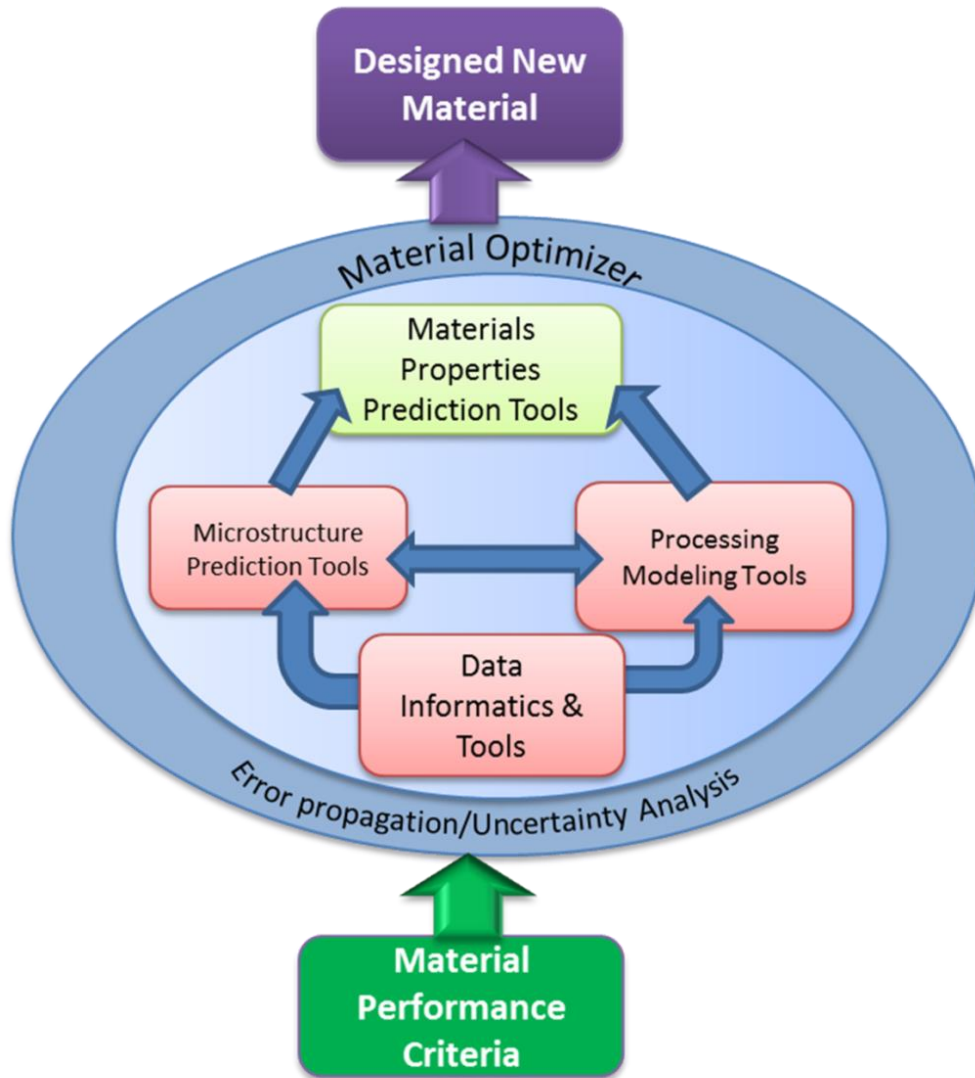
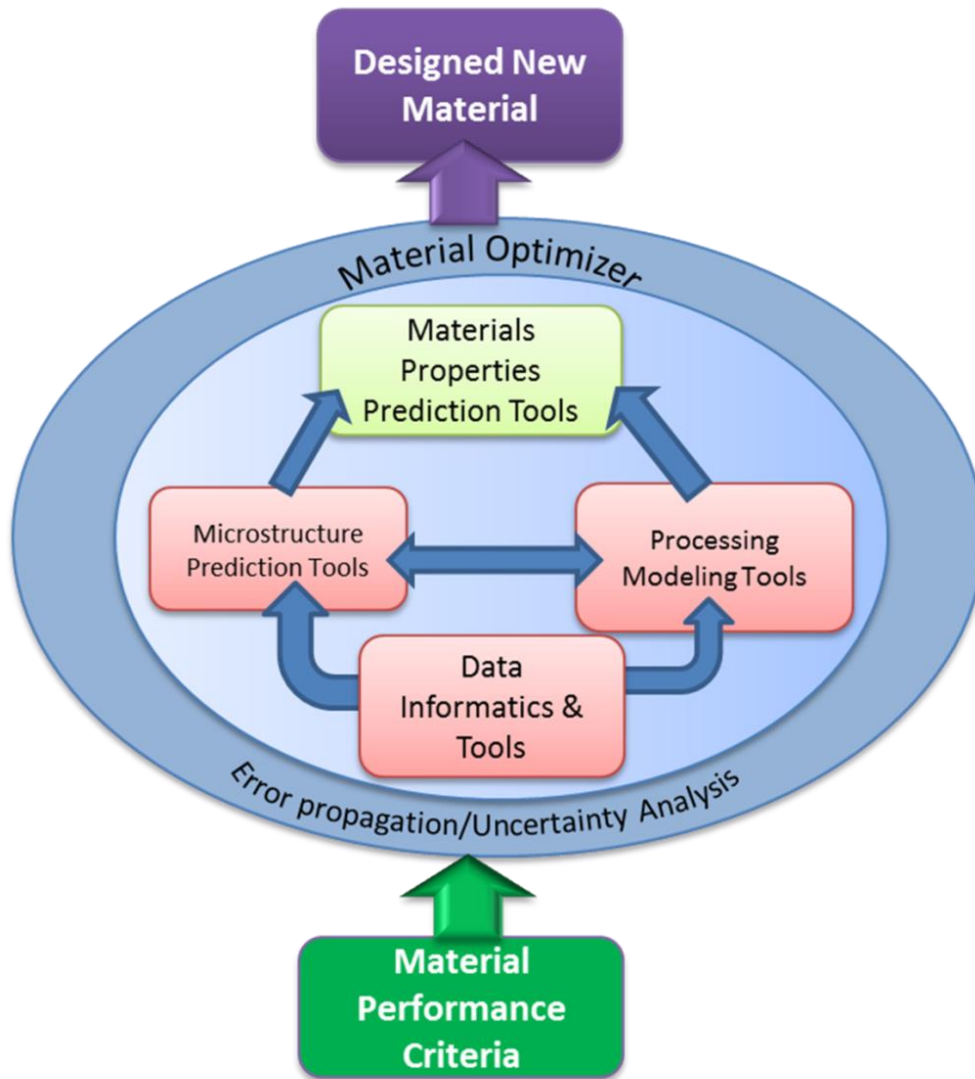


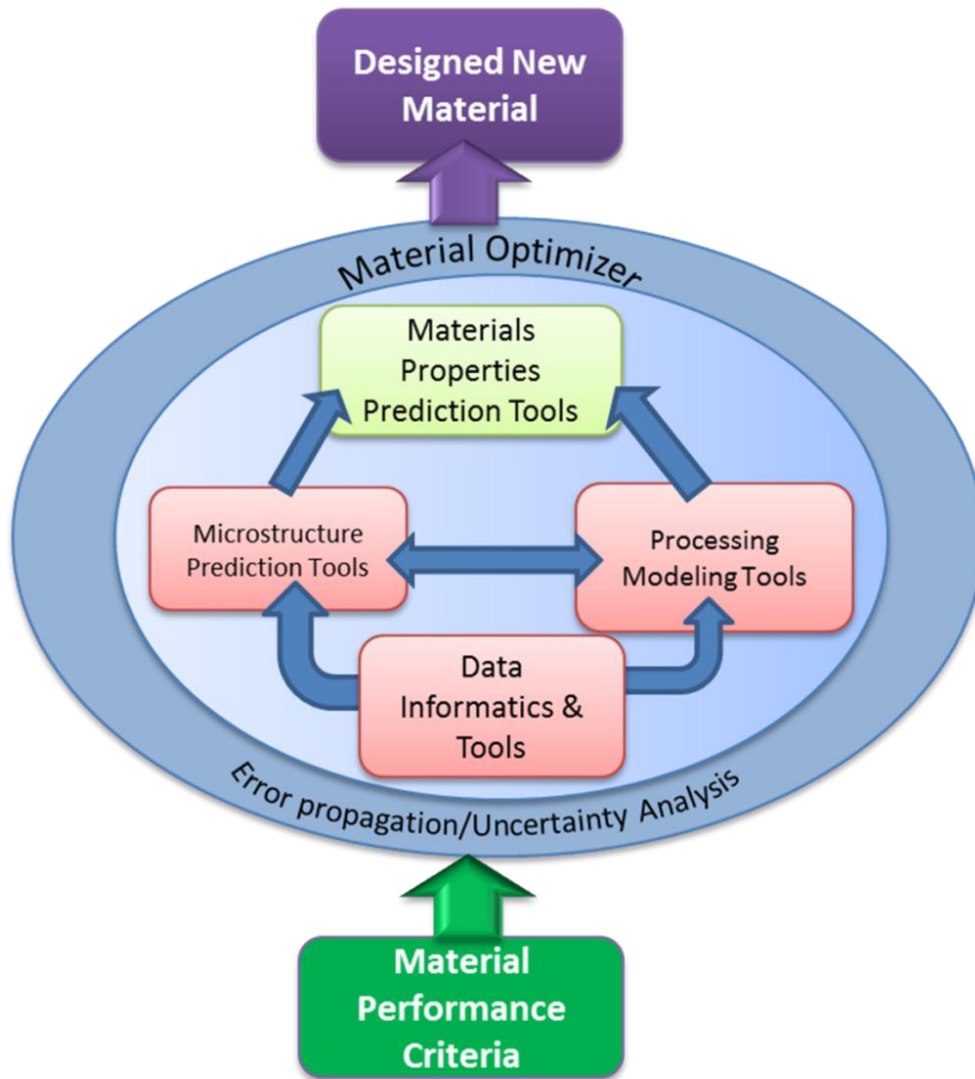
# Requirements





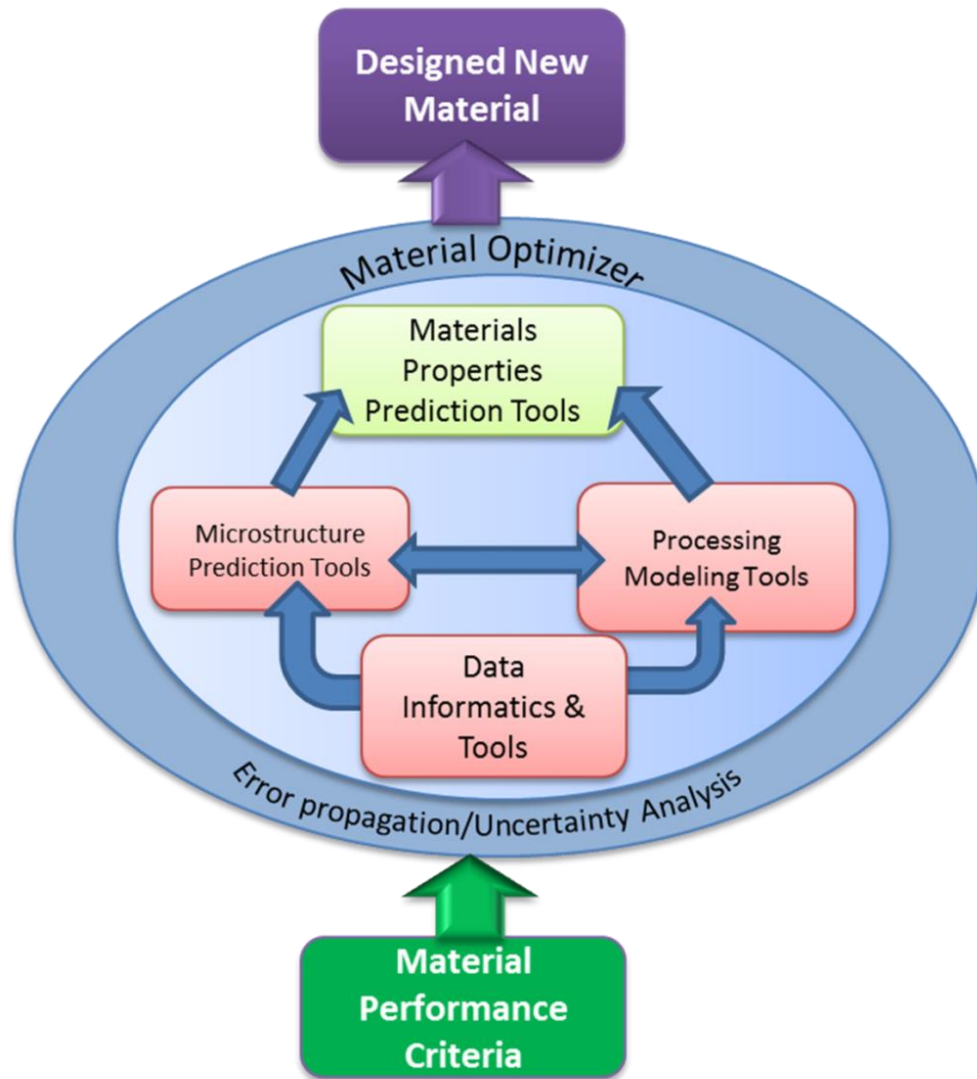
## Requirements

### 1. "DATA"



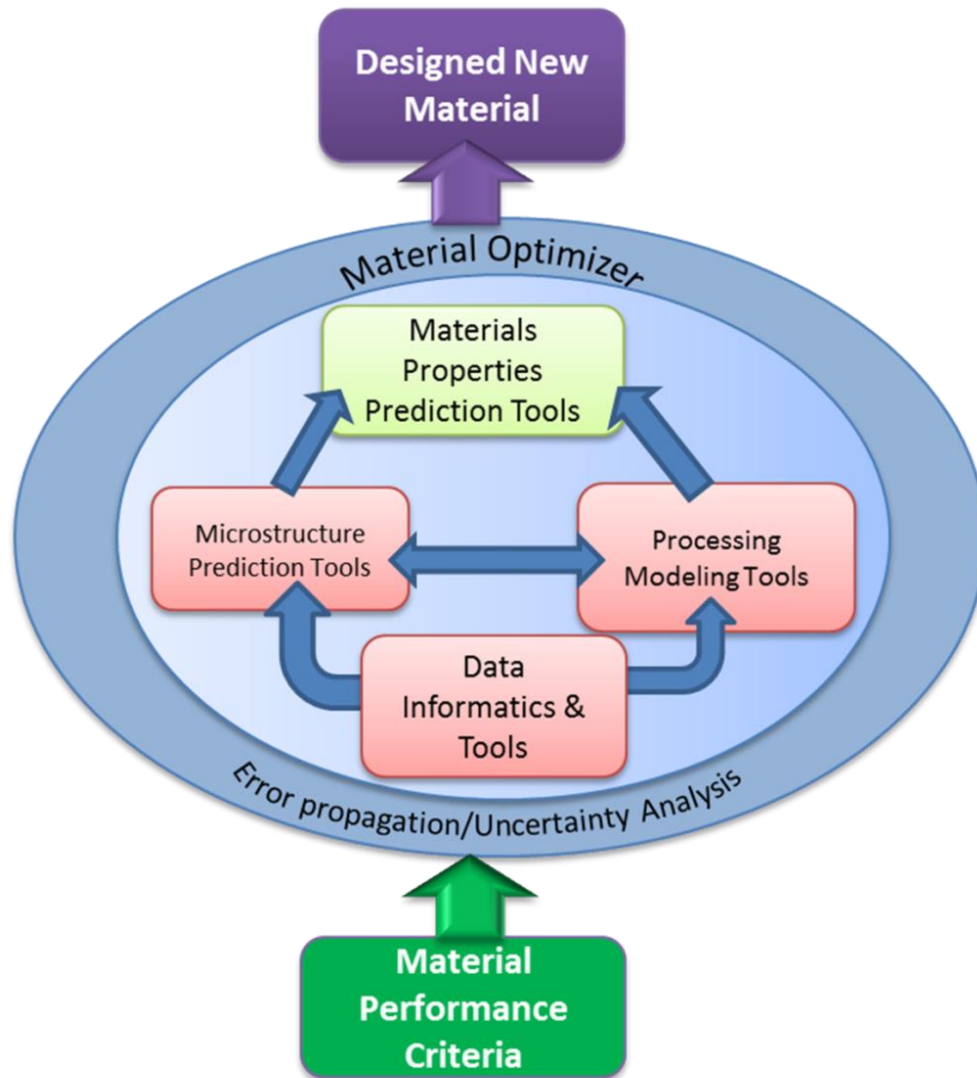
## Requirements

1. "DATA"
2. Interdisciplinary tools



## Requirements

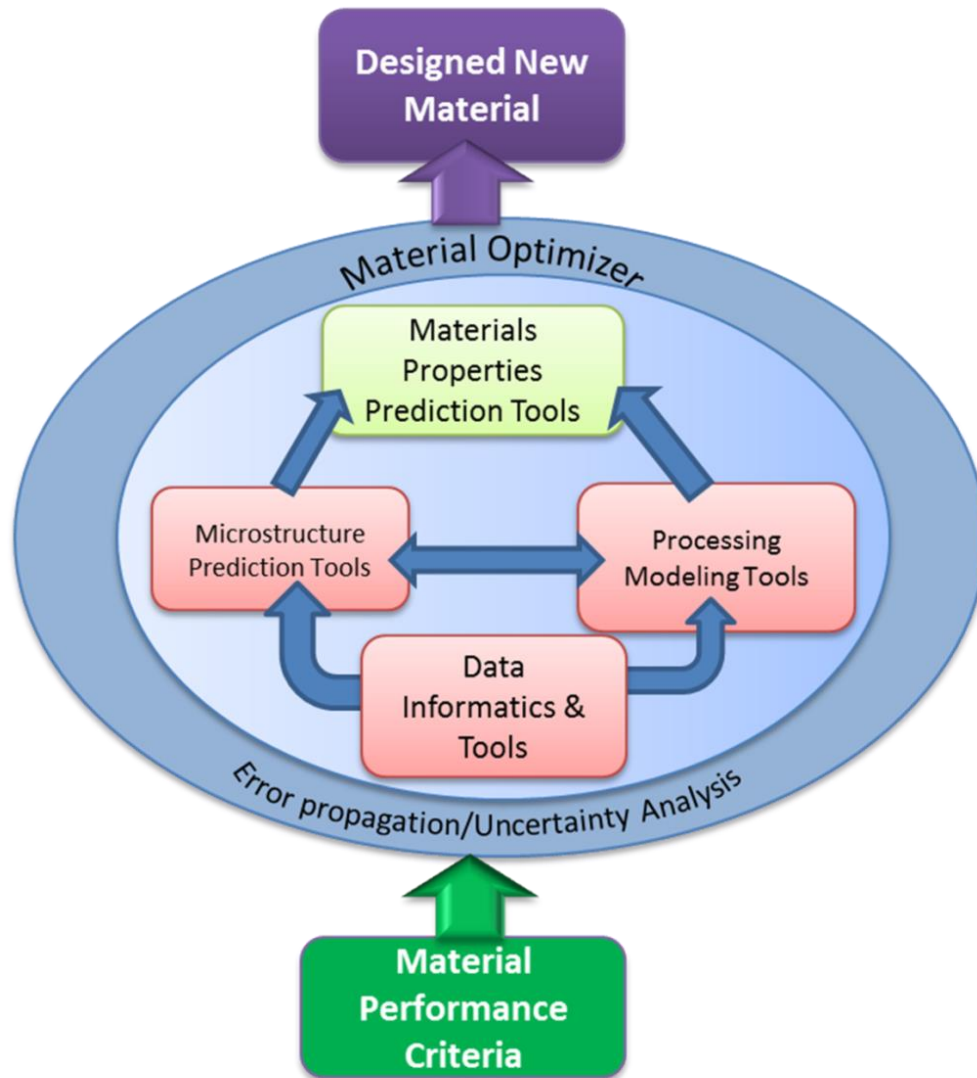
1. "DATA"
2. Interdisciplinary tools
3. Effective optimizer



## Requirements

1. "DATA"
2. Interdisciplinary tools
3. Effective optimizer

## Demands

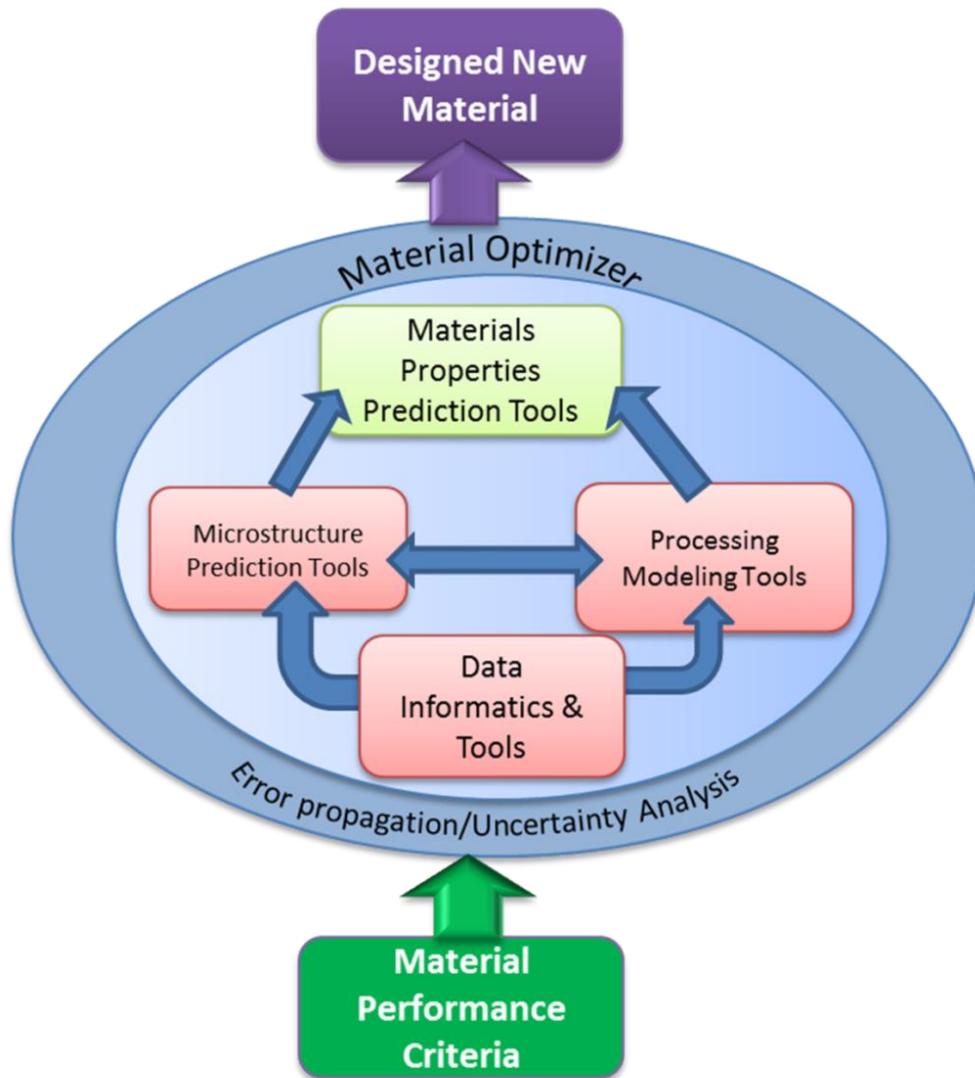


## Requirements

1. "DATA"
2. Interdisciplinary tools
3. Effective optimizer

## Demands

1. Low computational cost



## Requirements

1. "DATA"
2. Interdisciplinary tools
3. Effective optimizer

## Demands

1. Low computational cost
2. Easy model-switching



# A computational framework for designing Ni-based superalloy

S. Li, U. Kattner, C. Campbell,  
D. Wheeler, A. Reid

*National Institute of Standards and Technology*

May. 14 2015

# Outline

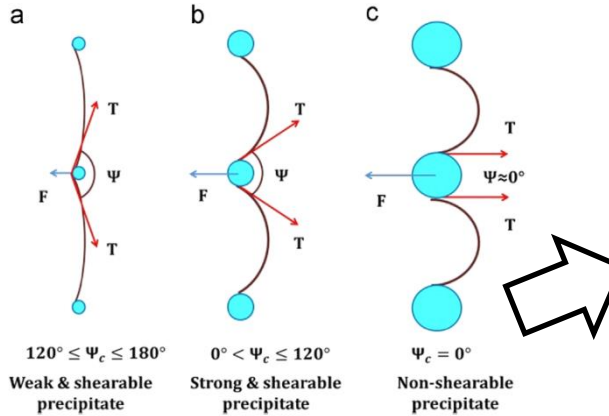
---

- ❖ Background:  $\gamma - \gamma'$  Ni Base Superalloy
- ❖ Computational Framework
  - Classical Nucleation, Growth and Coarsening Models
  - Elastic Deformation: Statistical tool, PyMKS
  - Plastic Deformation: Kocks-Mecking & energy conservation models
  - Optimization
- ❖ Summary

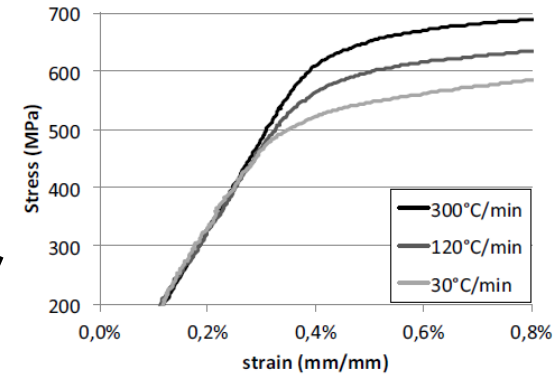
# $\gamma - \gamma'$ Ni-Base Superalloy

Olson, 1997  
 Ahmadi et al., 2014  
 Le Baillif et al., 2014

- $\gamma$  and  $\gamma'$  microstructure
- $\gamma'$  strengthening
- Chemistry & geometry properties affect performance
- Optimum composition & processing conditions are required

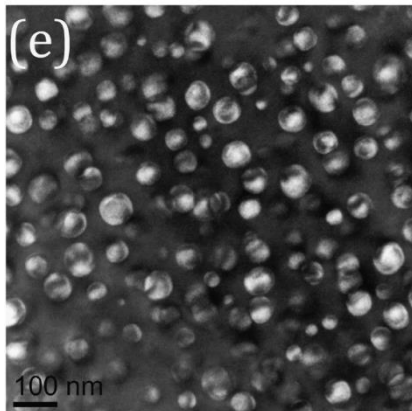


b) Tensile tests at 850°C

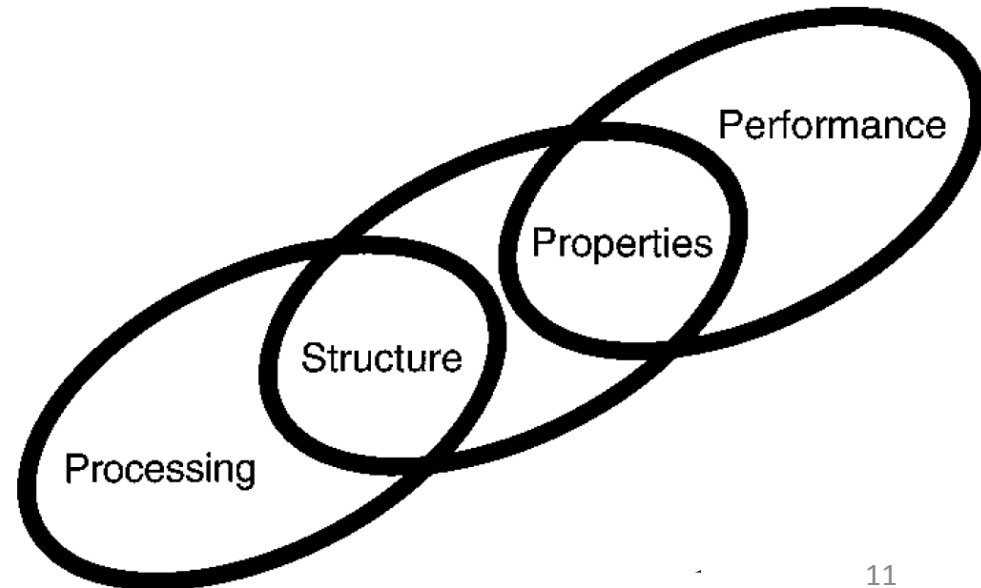


High Temperature Application

Precipitation hardening



$\gamma/\gamma'$  Microstructure



**Optimizer**

**Process-Structure**

**Structure-Property**

**Equilibrium Calculation**  
Phase Info., Incubation Time

Optimizer

Process-Structure

Structure-Property

**Optimizer**

**Equilibrium Calculation**  
Phase Info., Incubation Time



**Nucleation Model**  
Number Density

**Process-Structure**

**Structure-Property**

Optimizer

**Equilibrium Calculation**  
Phase Info., Incubation Time

**Nucleation Model**  
Number Density

**Growth/Coarsening Models**  
Radius & Total Volume Fraction  $\gamma'$

Process-Structure

Structure-Property

Optimizer

**Equilibrium Calculation**  
Phase Info., Incubation Time

**Nucleation Model**  
Number Density

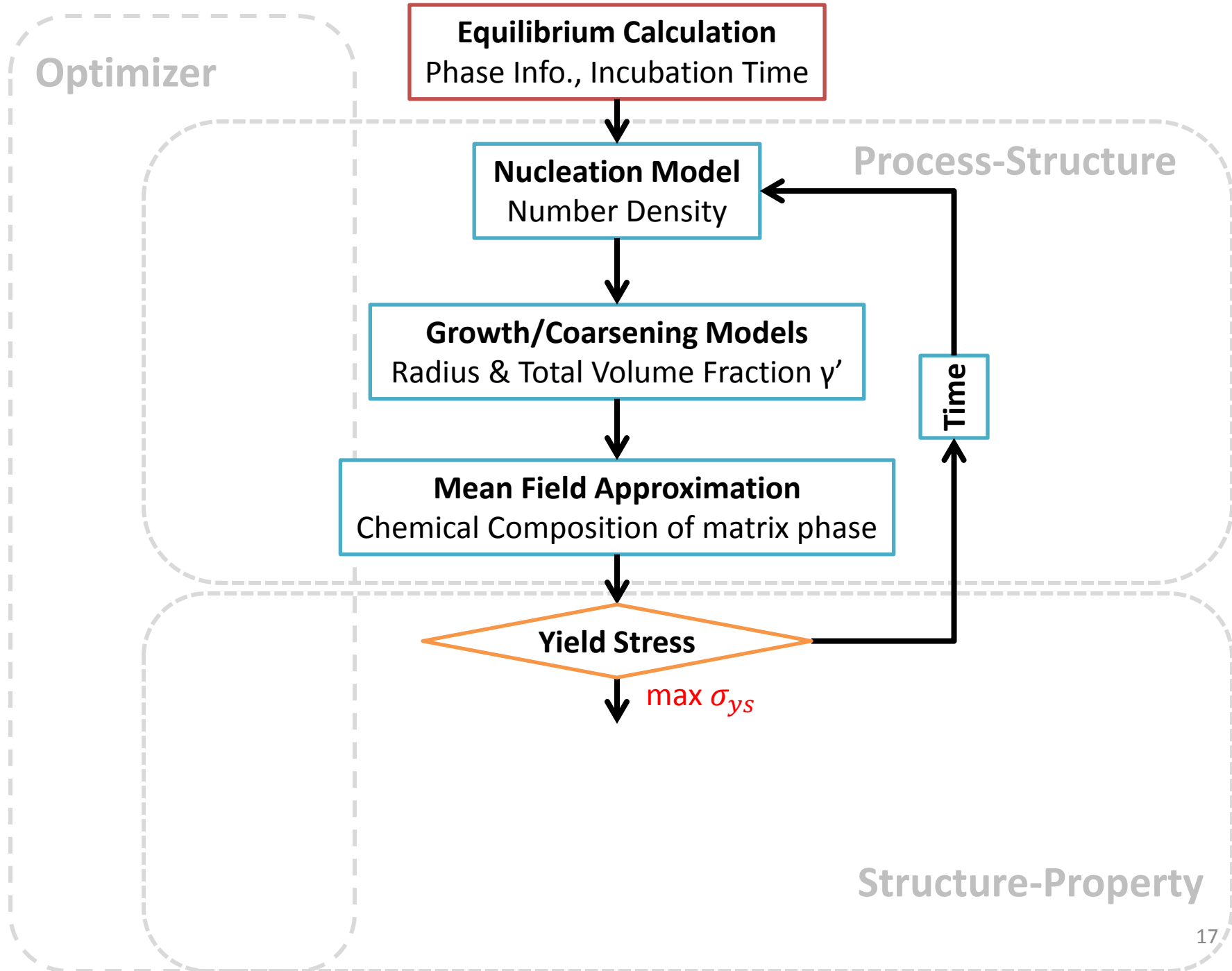
**Growth/Coarsening Models**  
Radius & Total Volume Fraction  $\gamma'$

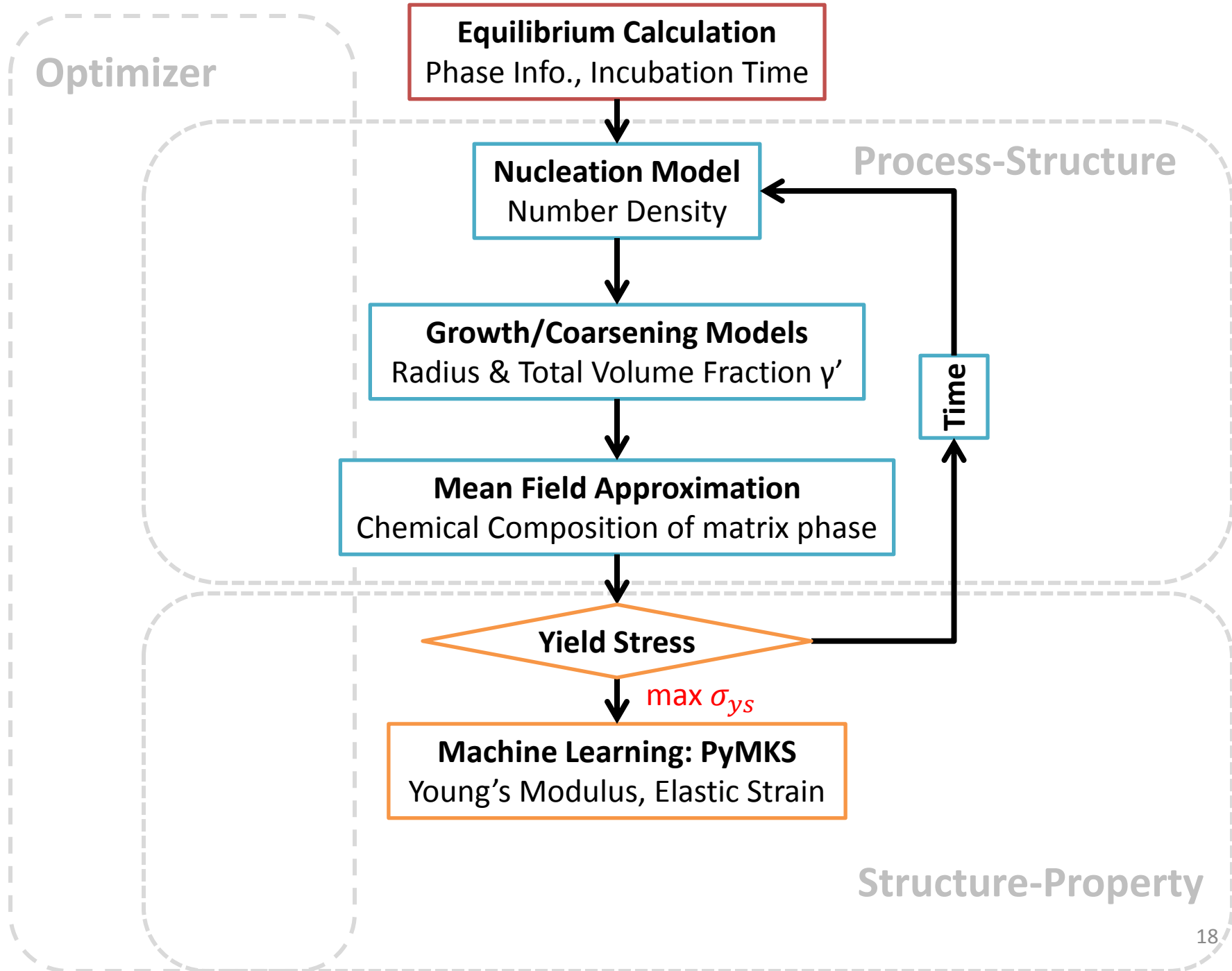
**Mean Field Approximation**  
Chemical Composition of matrix phase

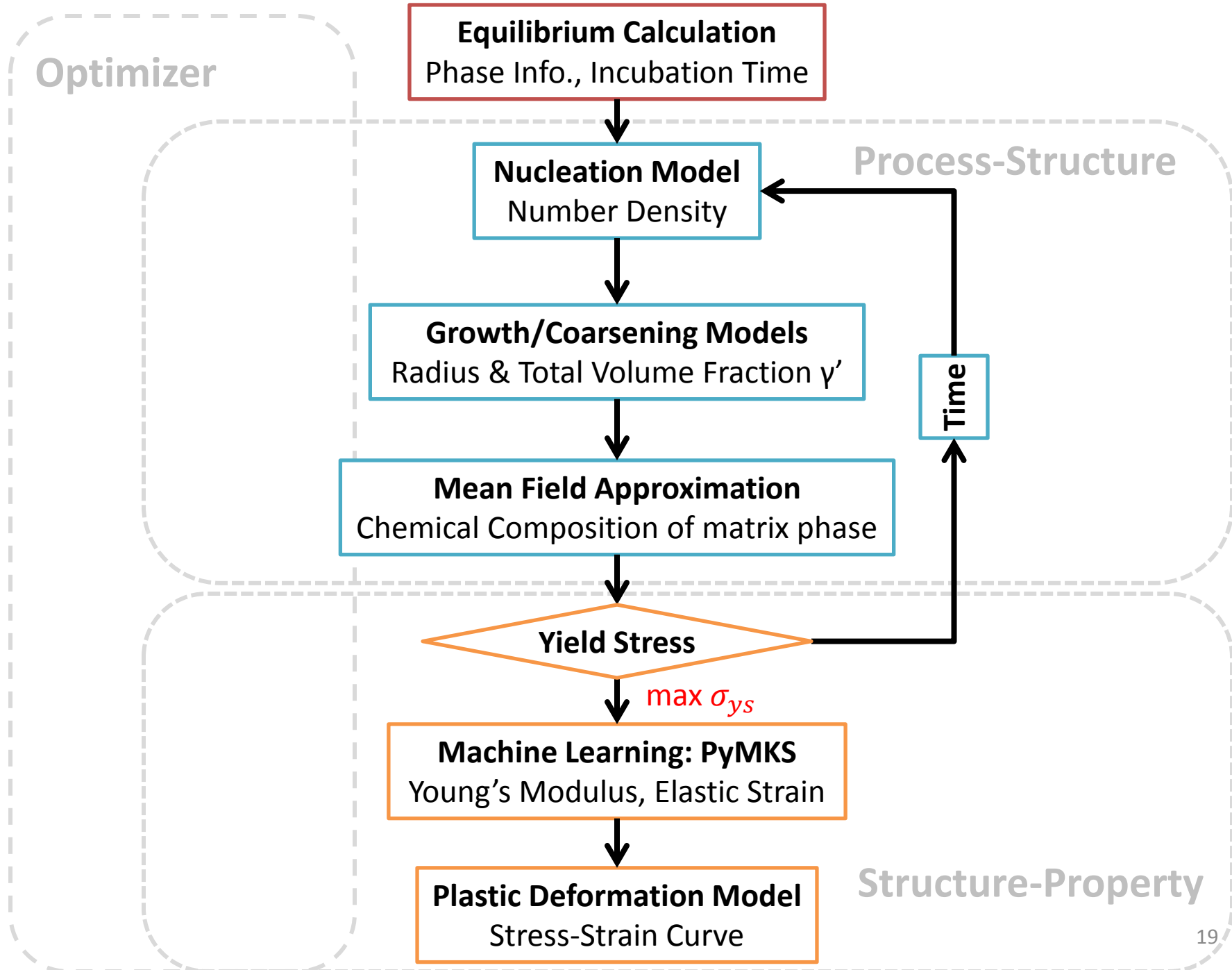
Process-Structure

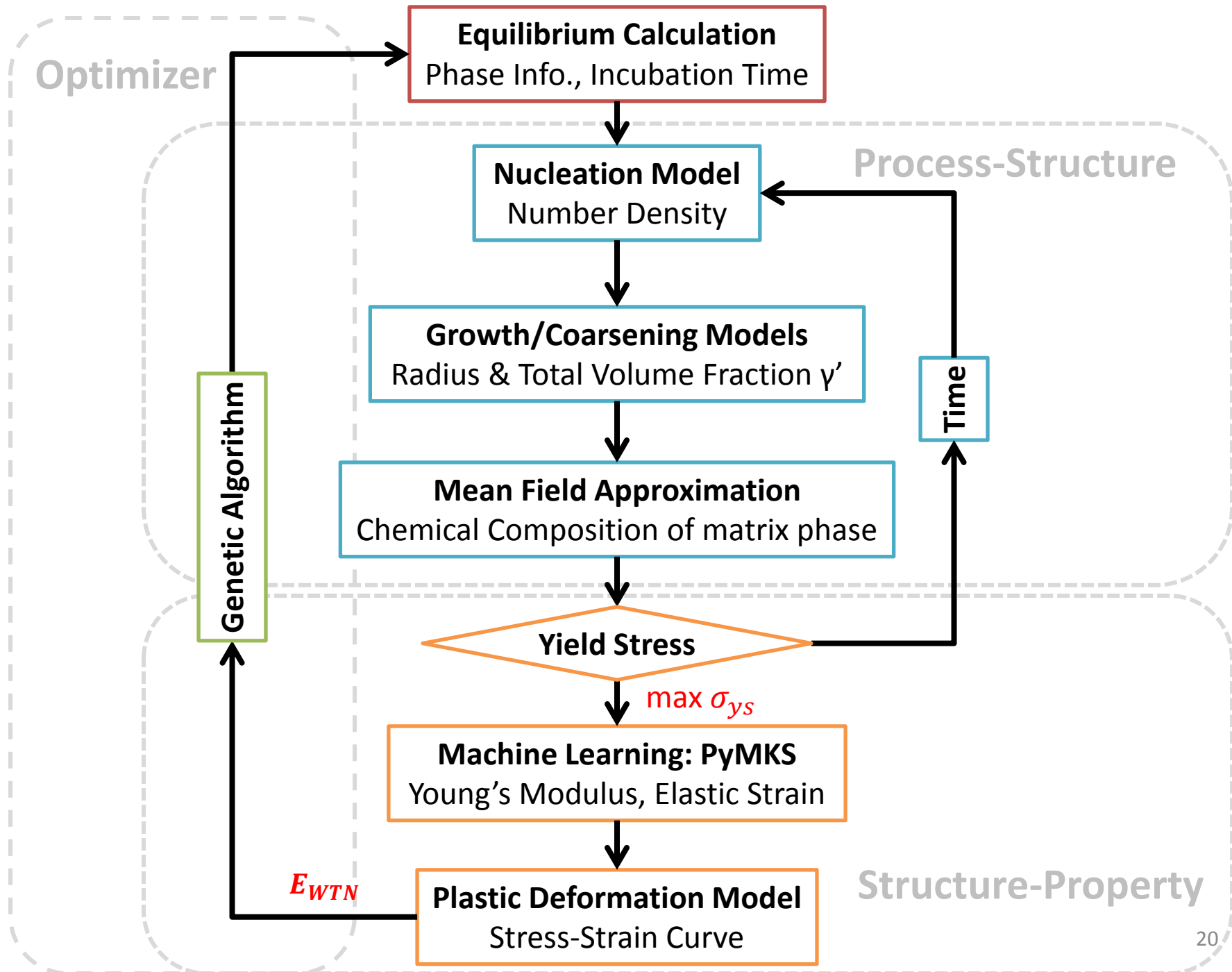
Structure-Property











# Homogeneous, NON-Steady-State Nucleation

Russell, 1978  
Wagner et al., 2001

$$\dot{N}(t) = Z\beta N_0 \exp\left(\frac{-\Delta G^*}{K_B T}\right) \exp\left(\frac{-\tau}{t}\right)$$

- Cluster size is estimated by Boltzmann distribution of total number of clusters,  $N_0$
- Interface energy ( $E_{INT}$ ) and  $N_0$  are the remaining parameters
- $\beta$  - rate of atom jumps from matrix to precipitate
- Zeldovich factor,  $Z$ , is employed to correct the equation
- The parameters are calculated using Thermo-Calc with TCNI6 database

$$\Delta G^* = \frac{16\pi E_{INT}^3}{3 \Delta G_N^2}$$

$$\Delta G_N = \frac{\Delta G_{ch}}{V_m^{\gamma'}} = -\frac{RT}{V_m^{\gamma'}} \sum_i \bar{C}_i^{\gamma'} \ln \frac{a_i}{\bar{a}_i^{\gamma}}$$

$$Z = \frac{V_M^\beta}{2\pi N_A r_0^2} \sqrt{\frac{E_{INT}}{K_B T}}$$

$$\beta = \frac{4\pi r_0^2}{a^4} \left[ \sum \frac{(\bar{C}_i^{\gamma'} - \bar{C}_i^{\gamma})^2}{\bar{C}_i^{\alpha} D_i} \right]^{-1}$$

$$r_0 = -\frac{2E_{INT} V_M^\beta}{\Delta G_N}$$

$$\tau = \frac{1}{\theta Z^2 \beta}$$

$\gamma'$  growth

$$\frac{dR}{dt} = \frac{D_i^{\gamma'}}{[1 - \lambda_j \sqrt{\pi} \exp(\lambda_j^2) \operatorname{erfc}(\lambda_j)] R} \frac{C_i^{\gamma'} - \bar{C}_i^{\gamma'}}{(\bar{C}_i^{\gamma'} - \bar{C}_i^{\gamma})}$$

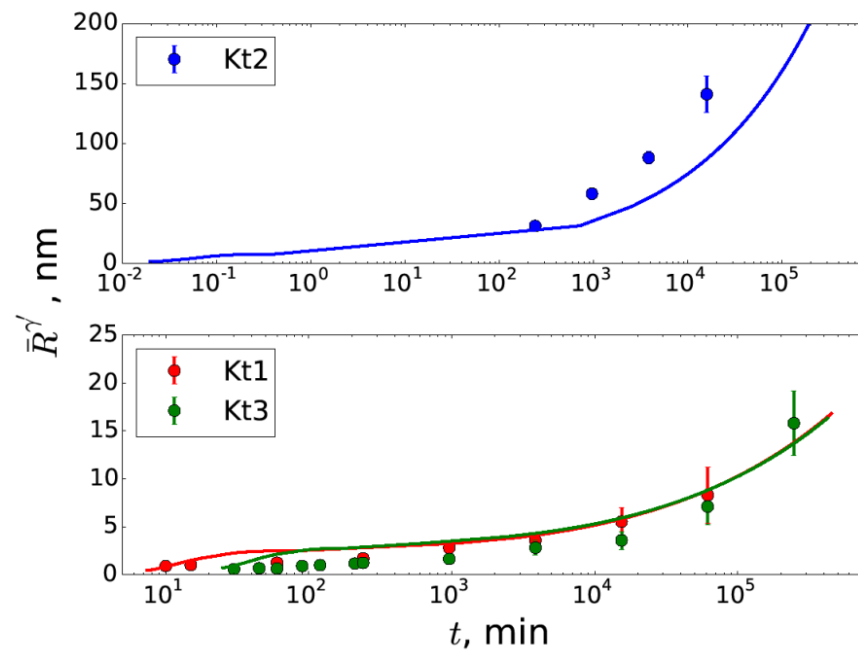
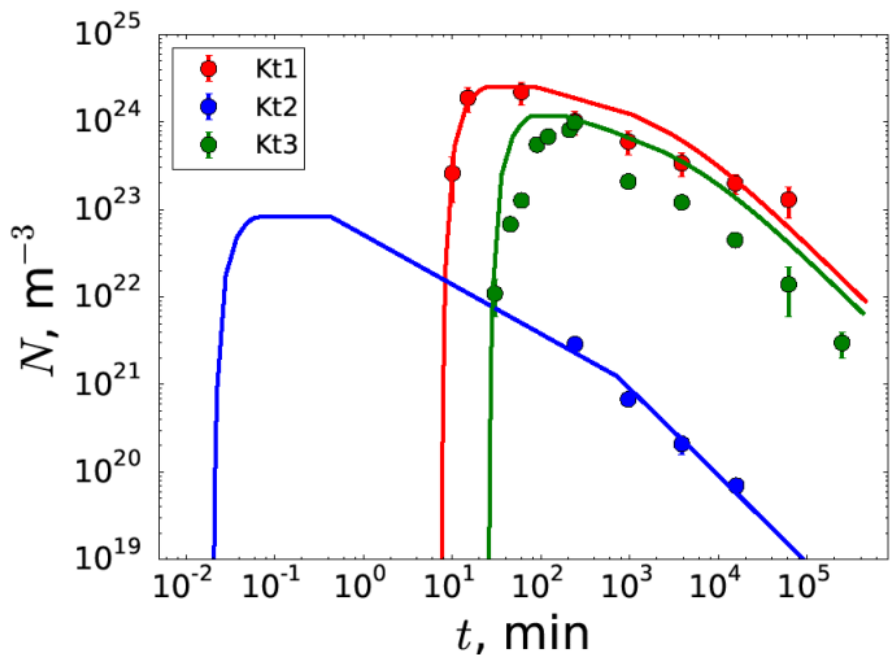
- $\bar{C}_i^{\gamma'}$  is taken as the equilibrium composition in  $\gamma'$
- $[1 - \lambda_j \sqrt{\pi} \exp(\lambda_j^2) \operatorname{erfc}(\lambda_j)] R$  stands the Effective Diffusion Distance

$\gamma'$  coarsening

$$\frac{dR}{dt} = \frac{8}{27} \frac{E_{INT} V_M^{\gamma'}}{R^2 N_A k_B T} \frac{D_i^{\gamma'} \bar{C}_i^{\gamma'}}{\bar{C}_i^{\gamma'} - \bar{C}_i^{\gamma}}$$

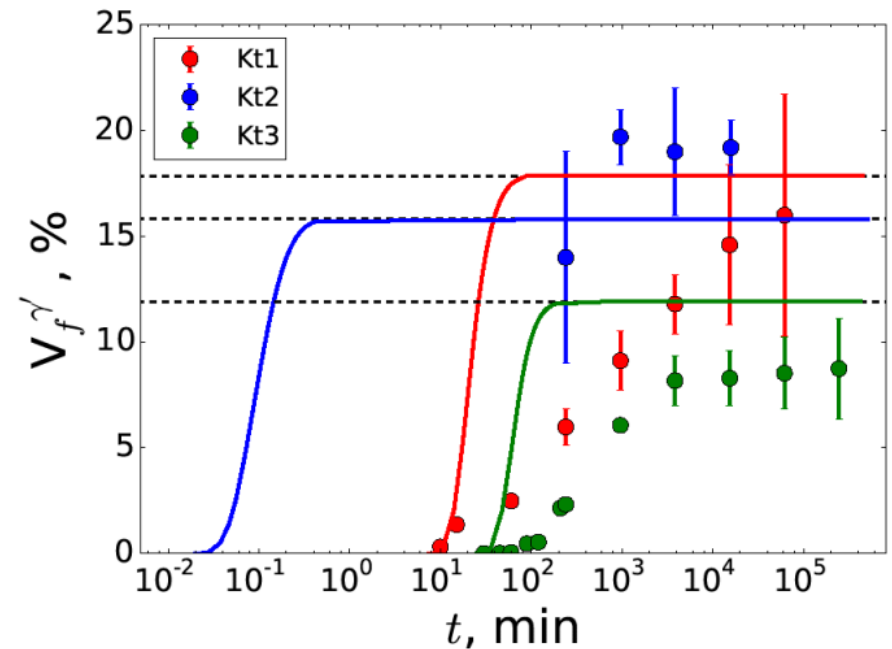
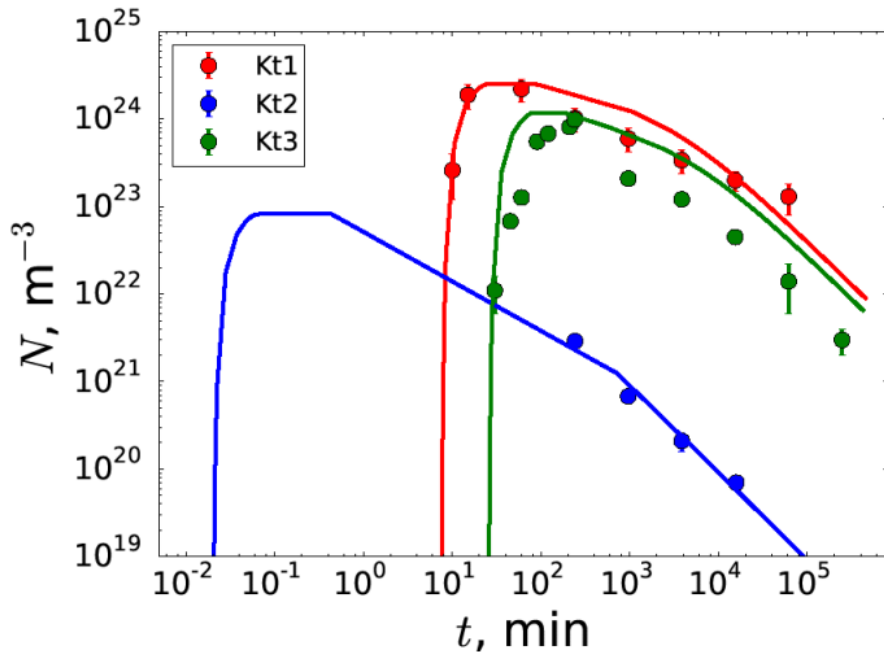
# Determine $E_{INT}$ and $N_0$

	Experimental			Data Regression	
	Composition, %	$T_p$ , K	reference	$E_{int}$ , mJ/m <sup>2</sup>	$N_0$ , 1/m <sup>2</sup>
Kt1	Ni-7.5Al-8.5Cr	873	Booth-Morrison et al., 2008	15	$1.5 \times 10^{26}$
Kt2	Ni-9.8Al-8.3Cr	1073	Sudbrack et al., 2008	24	$5 \times 10^{27}$
Kt3	Ni-6.5Al-9.5Cr	873	Booth-Morrison et al., 2010	18	$4.0 \times 10^{26}$



# Determine $E_{INT}$ and $N_0$

	Experimental			Data Regression	
	Composition, %	$T_p$ , K	reference	$E_{int}$ , mJ/m <sup>2</sup>	$N_0$ , 1/m <sup>2</sup>
Kt1	Ni-7.5Al-8.5Cr	873	Booth-Morrison et al., 2008	15	$1.5 \times 10^{26}$
Kt2	Ni-9.8Al-8.3Cr	1073	Sudbrack et al., 2008	24	$5 \times 10^{27}$
Kt3	Ni-6.5Al-9.5Cr	873	Booth-Morrison et al., 2010	18	$4.0 \times 10^{26}$





# Determine $E_{INT}$

Nishizawa et al., 2001  
Li et al., 2002

Nishizawa et al., 2001

$$E_{int} = \alpha |\Delta H^{\gamma \rightarrow \gamma'}|$$

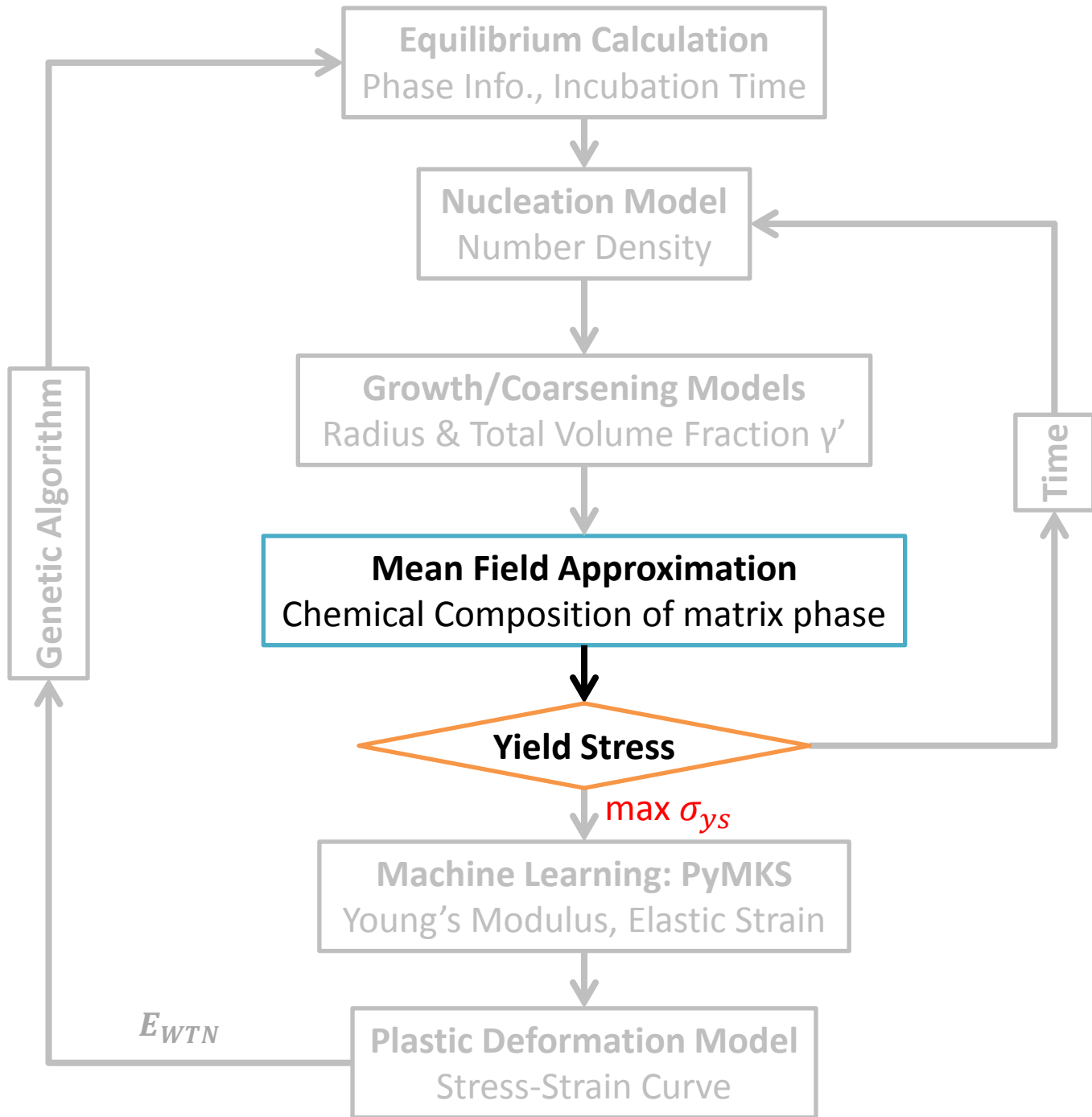
$$E_{int} \text{ \& } |\Delta H^{\gamma \rightarrow \gamma'}|$$

$$\alpha = f(T_p)$$

$$\alpha = (3.75 \times 10^{-2} T_p - 2.23) \times 10^{-6}$$

	Experimental		Computation	Parameter		
	Composition %	$T_p$ Kelvin	$ \Delta H^{\gamma \rightarrow \gamma'} $ $10^4$ J/mol	$E_{int}$ mJ/m <sup>2</sup>	$\alpha$ $10^{-6}$ mol/m <sup>2</sup>	$E_{int,cal}$ mJ/m <sup>2</sup>
Kt1	Ni-7.5Al-8.5Cr	873	1.52	15	0.99	15.
Kt2	Ni-9.8Al-8.3Cr	1073	1.34	24	1.80	24
Kt3	Ni-6.5Al-9.5Cr	873	1.64	18	1.10	17.1

$$E_{int} = (3.75 \times 10^{-2} T_p - 2.23) \times 10^{-6} |\Delta H^{\gamma \rightarrow \gamma'}|$$



# Yield Stress

Thomas et al., 2006

Roth et al., 1997

Reed., 2006

Collins et al., 2014

$$\sigma_{YS} = \sigma_0 + \sigma_{SS} + \sigma_{H-P} + \sqrt{\sigma_{\rho,0}^2 + \sigma_p^2}$$

- Calculations using results from previous steps:  $Vf_{\gamma'}$ ,  $r_{\gamma'}$ , and composition of matrix
- Lattice friction ( $\sigma_0$ ), solid solution ( $\sigma_{SS}$ ) and Hall-Petch effect ( $\sigma_{H-P}$ ) to yield stress is estimated [Roth97].
- $\sigma_p$  follows the minimum value among  $\sigma_{wc}$ ,  $\sigma_{sc}$  and  $\sigma_{or}$ .
- $E_{APB}$  is calculated

$$\sigma_{wc} = M \frac{E_{APB}}{2b} \left[ \left( \frac{6\bar{R}^{\gamma'} E_{APB} V_f^{\gamma'}}{\pi L_T} \right)^{0.5} - V_f^{\gamma'} \right]$$

$$\sigma_{sc} = 0.22M \left( \frac{\mu b}{\bar{R}^{\gamma'}} \right) \left( \frac{\pi \bar{R}^{\gamma'} E_{APB} V_f^{\gamma'}}{L_T} - V_f^{\gamma'} \right)^{0.5}$$

$$\sigma_{or} = M \frac{\mu b}{\bar{R}^{\gamma'}} \sqrt{\frac{V_f^{\gamma'}}{\pi}}$$

# APB Energy

$$E_{APB,[111]} = \frac{W_1 - 3W_2 + 4W_3 \dots}{\sqrt{3}(a\gamma')^2}$$

## Atomic Bonding Energies

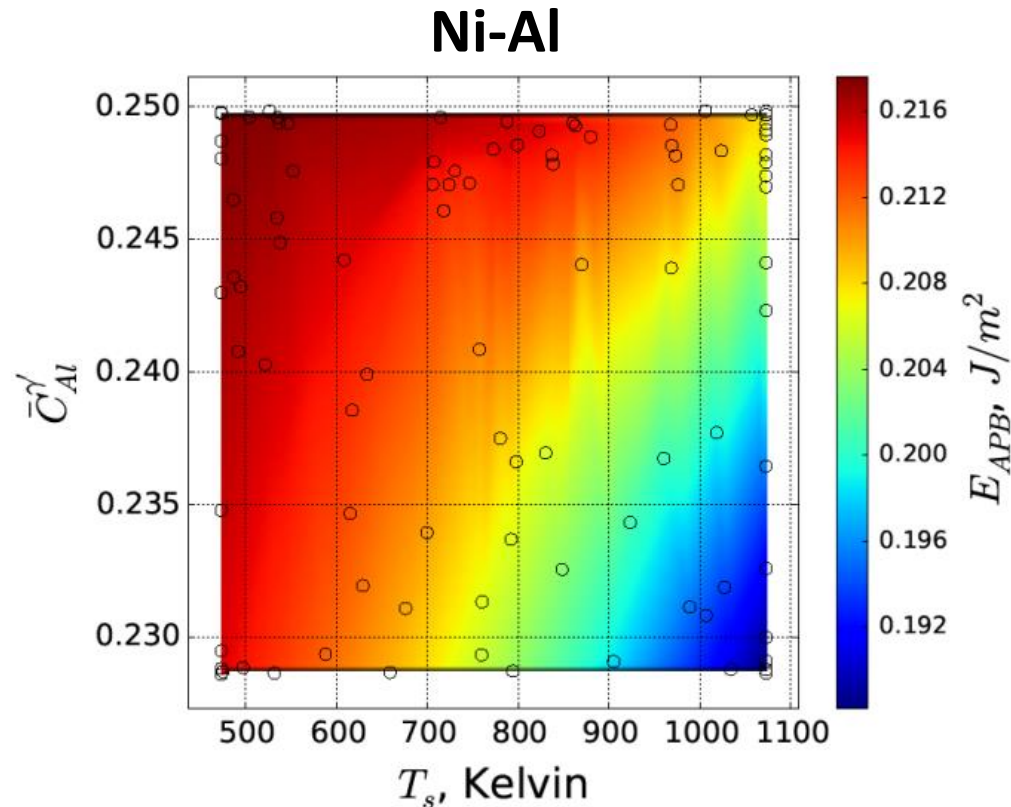
$$W_1 = 0.75W_{13}$$

$$W_2 = \frac{\Delta H^{ORD} (1 - \bar{C}_s^{\gamma'}) - \bar{C}_s^{\gamma'} \Delta H^{FCC}}{12Rc^2 (1 - \bar{C}_s^{\gamma'})}$$

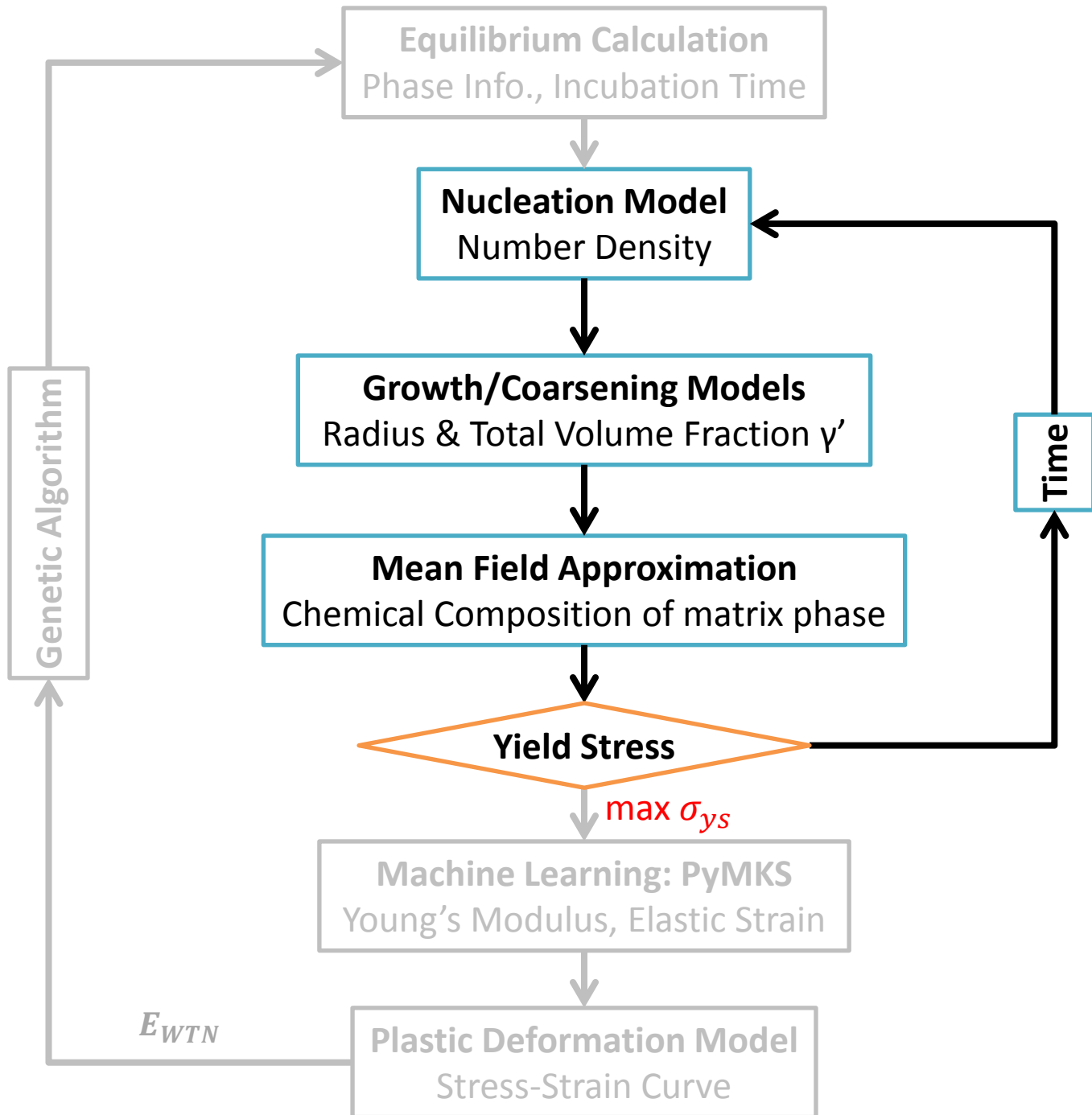
$$W_3 = 0.125W_{13}$$

$$W_{13} = \frac{3\Delta H^{FCC} + \Delta H^{ORD} \frac{(1 - \bar{C}_s^{\gamma'})}{\bar{C}_s^{\gamma'}}}{24Rc (1 - \bar{C}_s^{\gamma'})}$$

$$= W_1 + 2W_3$$

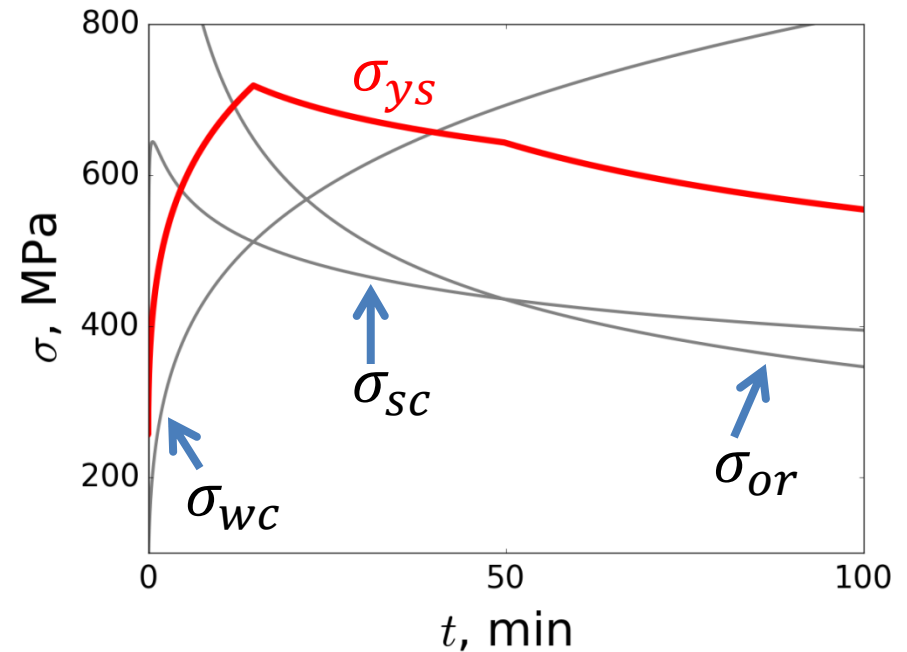
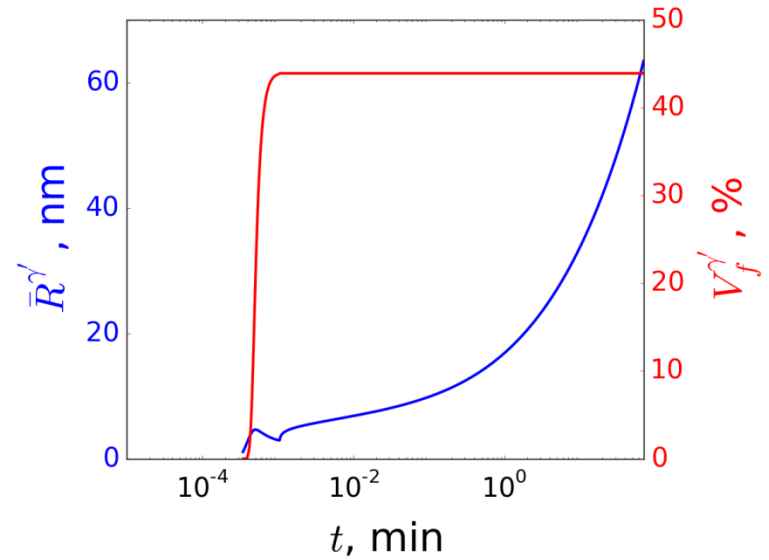


- Chemical composition  $\bar{C}_{Al}^{\gamma'}$ ,  $\bar{C}_{Cr}^{\gamma'}$  and lattice parameter of  $a\gamma'$  are calculated under equilibrium condition at  $T_p$
- Chemical properties are obtained at  $T_s$
- Chemical property of **Ni-Al-Cr** gives  $E_{APB,[111]} = 0.06-0.18 \text{ J/m}^2$



# Process-Structure-Yield Stress

$C_{Al}, \%$	13.62
$C_{Cr}, \%$	17.46
$T_p, \text{Kelvin}$	1230
$V_f^{\gamma'}, \%$	43.89
$E_{int}, \text{mJ/m}^2$	25.51
$E_{APB}, \text{mJ/m}^2$	118

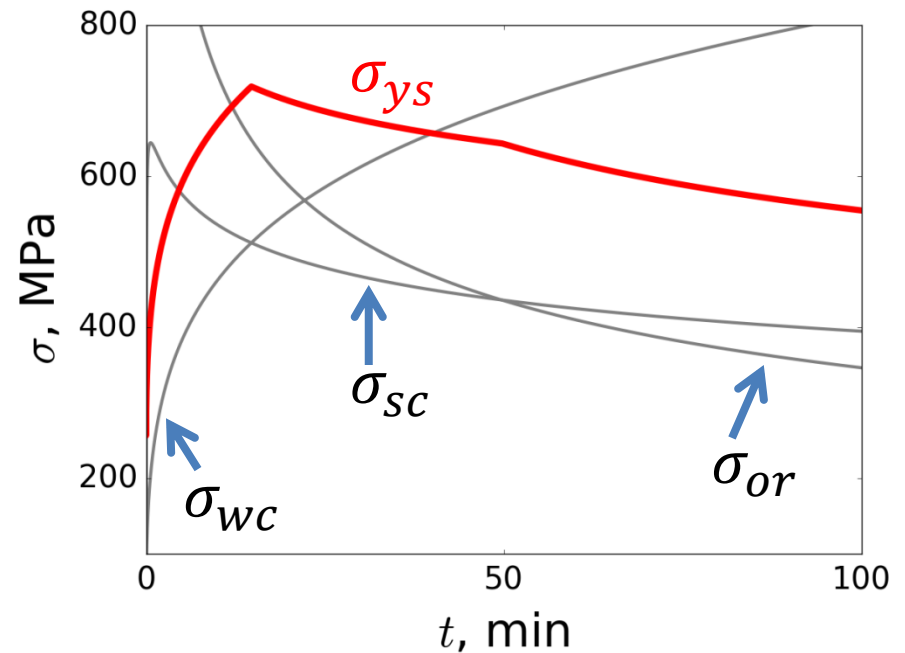
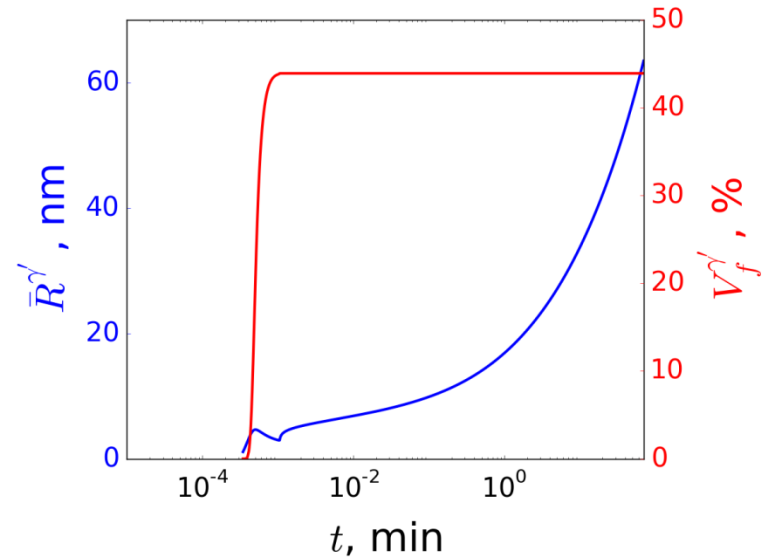


# Process-Structure-Yield Stress

$C_{Al}, \%$	13.62
$C_{Cr}, \%$	17.46
$T_p, \text{Kelvin}$	1230
$V_{f,max}^{\gamma'}, \%$	43.89
$E_{int}, \text{mJ/m}^2$	25.51
$E_{APB}, \text{mJ/m}^2$	118

Average radius

$$\bar{R}^{\gamma'} = \frac{\sum N_c R_c^{\gamma'}}{\sum N_c}$$

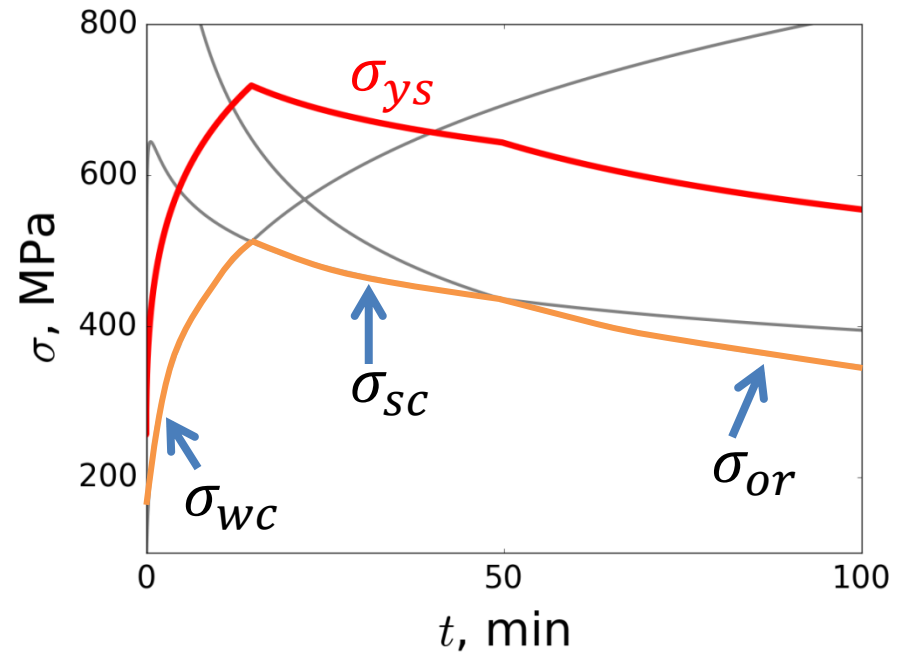
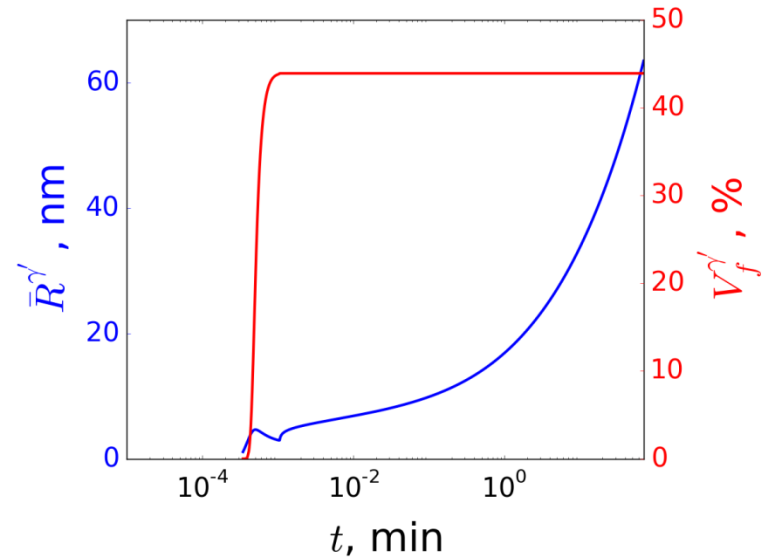


# Process-Structure-Yield Stress

$C_{Al}, \%$	13.62
$C_{Cr}, \%$	17.46
$T_p, \text{Kelvin}$	1230
$V_{f,max}^{\gamma'}, \%$	43.89
$E_{int}, \text{mJ/m}^2$	25.51
$E_{APB}, \text{mJ/m}^2$	118

Average radius

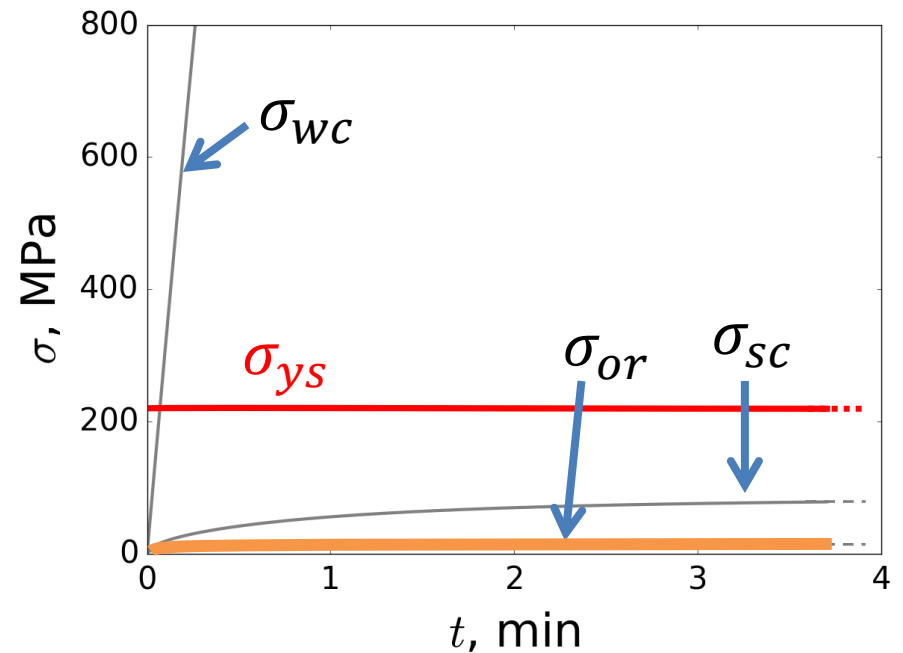
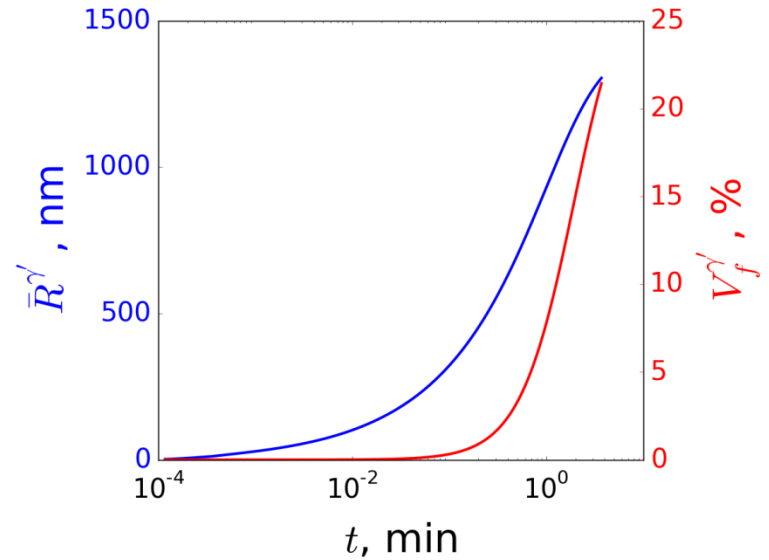
$$\bar{R}^{\gamma'} = \frac{\sum N_c R_c^{\gamma'}}{\sum N_c}$$

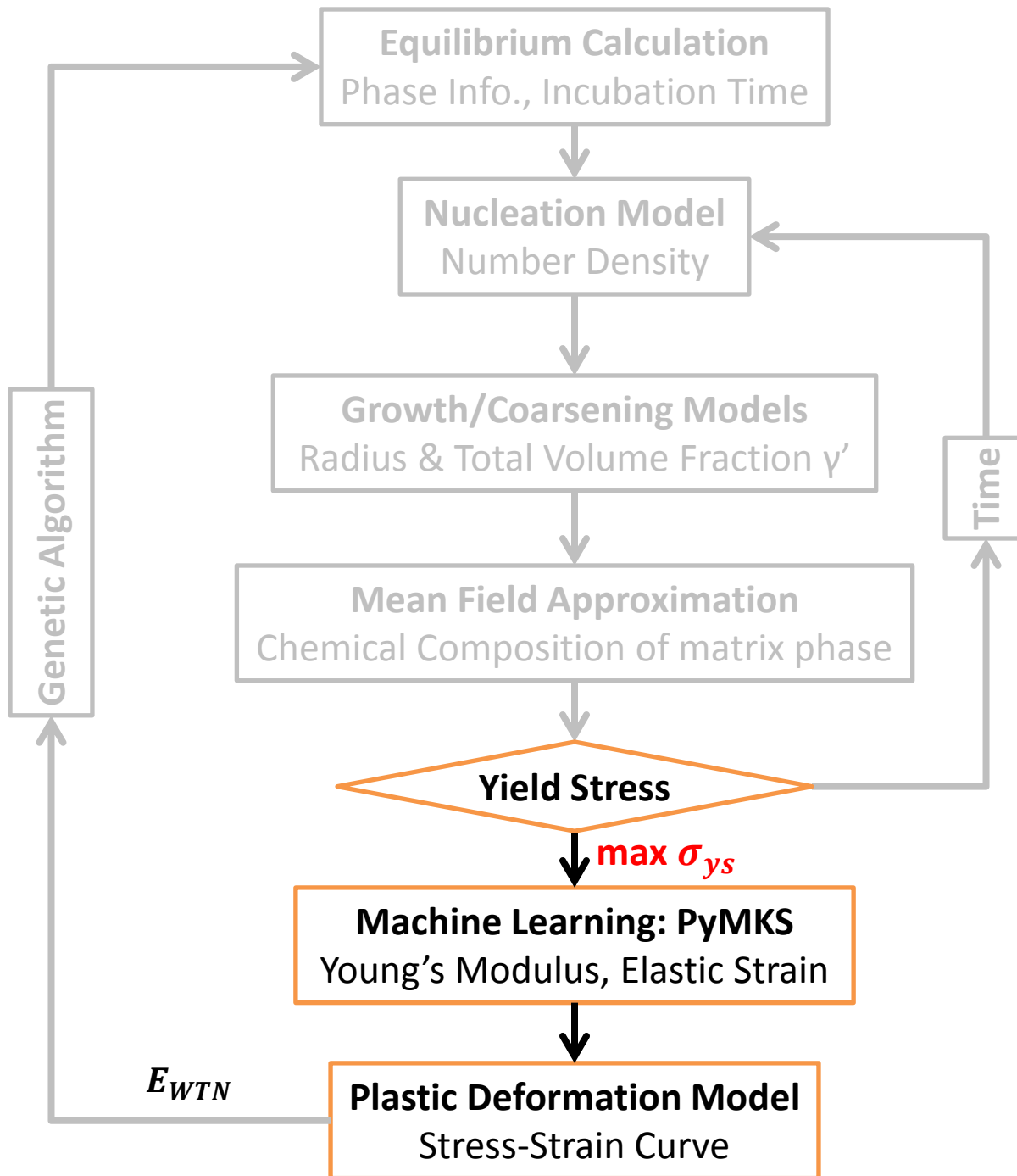




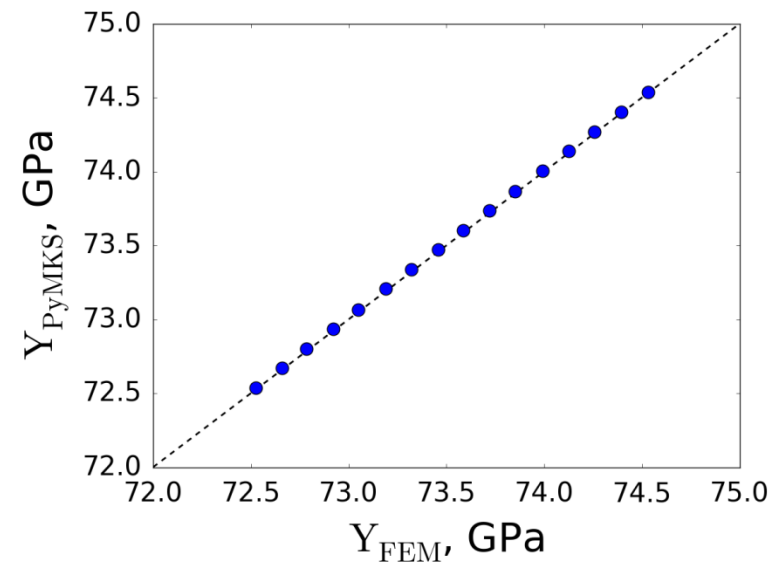
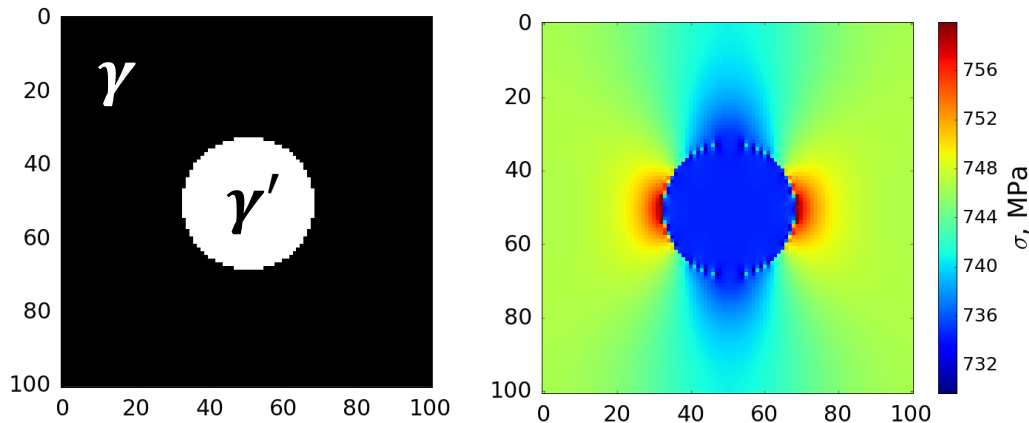
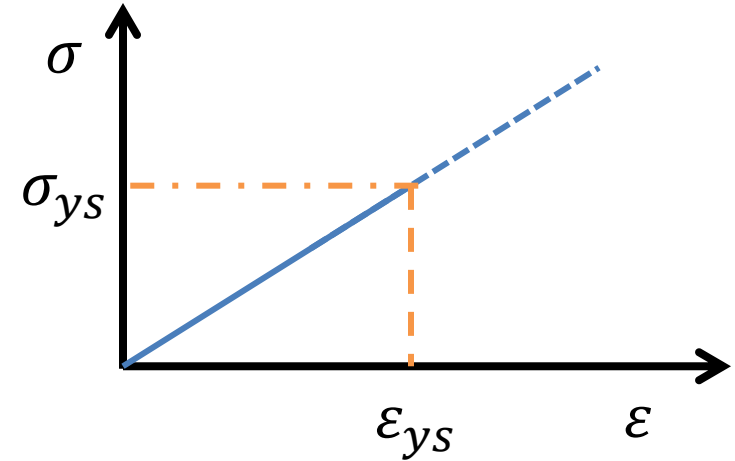
# Process-Structure-Yield Stress

$C_{Al}, \%$	14.05
$C_{Cr}, \%$	10.16
$T_p, \text{Kelvin}$	1328
$V_f^{\gamma'}$ , %	26.31
$E_{int}, \text{mJ/m}^2$	27.47
$E_{APB}, \text{mJ/m}^2$	157





- Statistical/machine learning tool correlating microstructure with properties by linear function
- By employing machine learning technique, PyMKS can reproduce the FEM calculations in a more efficient way
- For the microstructure with high volume fraction of  $\gamma'$ , the representative volume element is created for PyMKS calculation



The evolution of the dislocation density ( $\rho$ ) is calculated as increasing strain based on non-equilibrium thermodynamics and Kocks-Mecking model using shear modulus ( $\mu$ ), burger's vector ( $b$ ), mean free path of dislocation ( $l$ ), vibration frequency ( $\nu_0$ ), energy barrier of dislocation annihilation ( $\Delta G_\rho$ ) and model constant ( $C, \alpha$ )

$$\rho_{in, \varepsilon + \Delta \varepsilon} = \rho_{in, \varepsilon} + \frac{(\mu b^2 + \tau b l) \frac{\nu_0}{\dot{\varepsilon}} \exp\left(-\frac{\Delta G_\rho}{kT}\right) \rho_{in, \varepsilon} - \tau_\rho}{\frac{1}{2} C \alpha \mu b^2 - (\mu b^2 + \tau b l)} \Delta \varepsilon$$

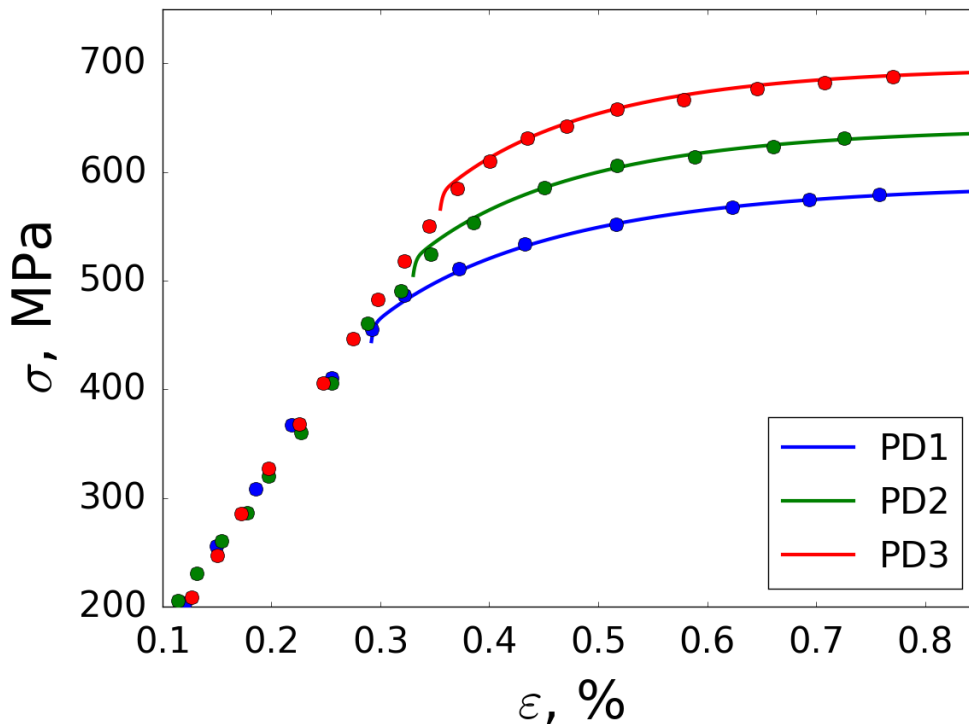


$\Delta \varepsilon$



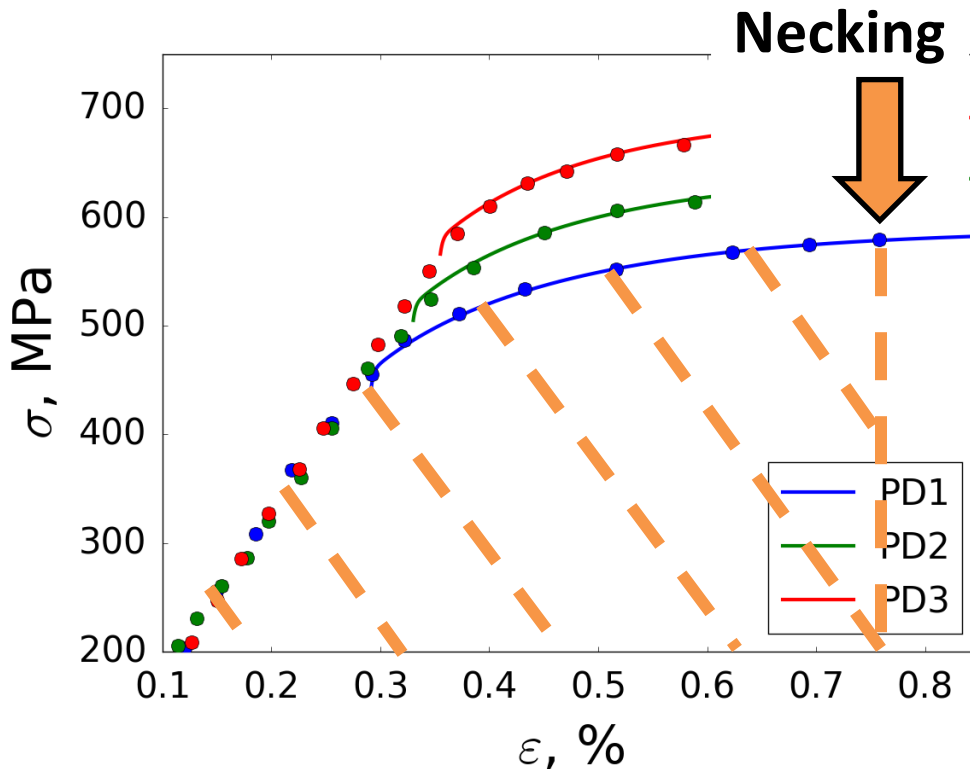
$$M\tau = \sigma_0 + \sigma_{SS} + \sigma_{H-P} + \sqrt{\sigma_\rho^2 + \sigma_p^2}$$

	$V_f \gamma'$	$\sigma_{ys}$ , MPa	$\varepsilon_{ys}$ , %
PD1	0.323	450	0.29
PD2	0.296	560	0.33
PD3	0.278	570	0.36

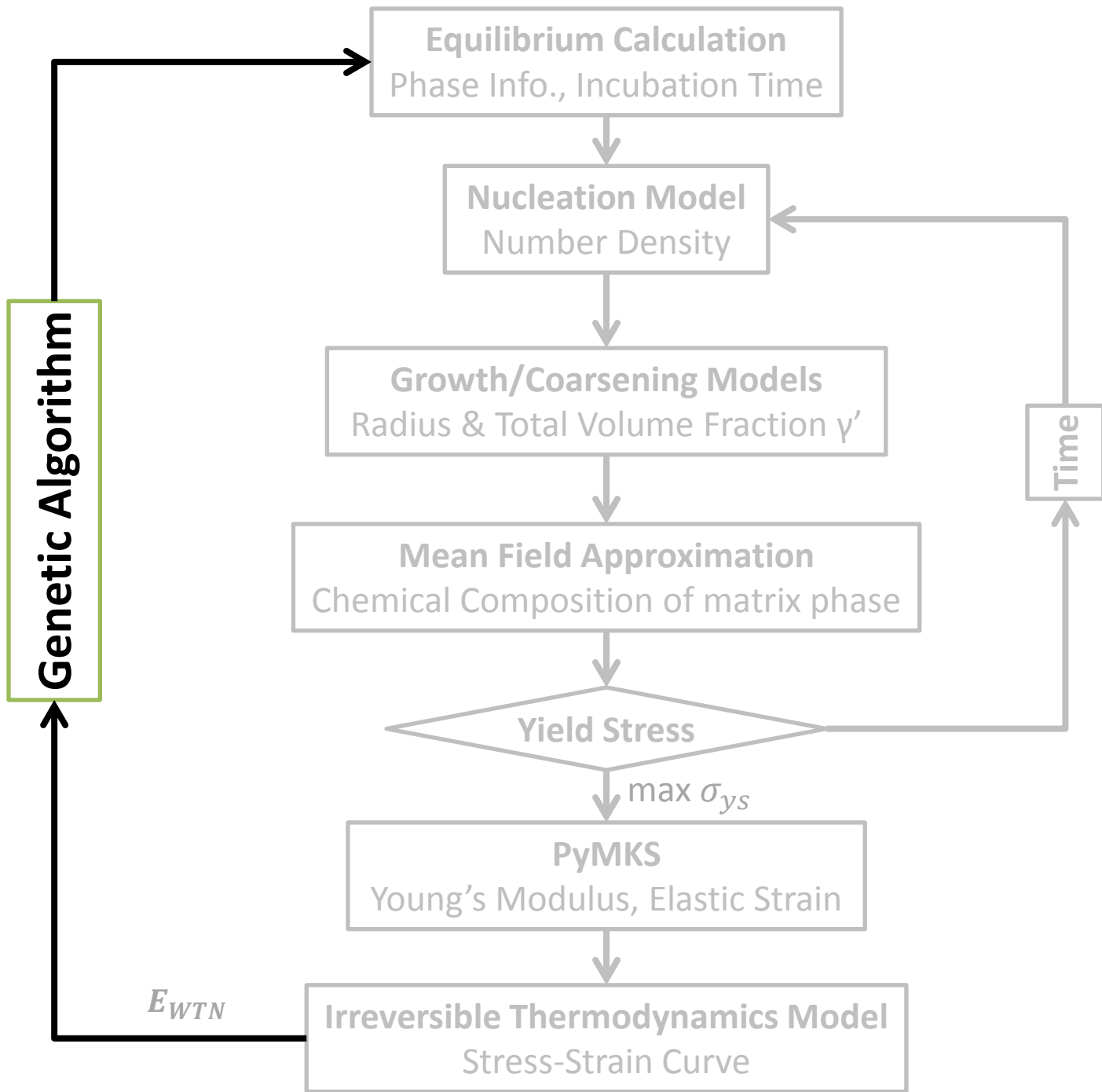


- $T_s = 1123K$
- PD1 is used for calibration
- $\Delta G_\rho = 3.08 \text{ eV}$  and  $C = -180$  provide the best agreement to PD1

	$V_f^{\gamma'}$	$\sigma_{ys}$ , MPa	$\epsilon_{ys}$ , %
PD1	0.323	450	0.29
PD2	0.296	560	0.33
PD3	0.278	570	0.36



- $T_s = 1123K$
- PD1 is used for calibration
- $\Delta G_\rho = 3.08 \text{ eV}$  and  $C = -180$  provide the best agreement to PD1



# Optimization

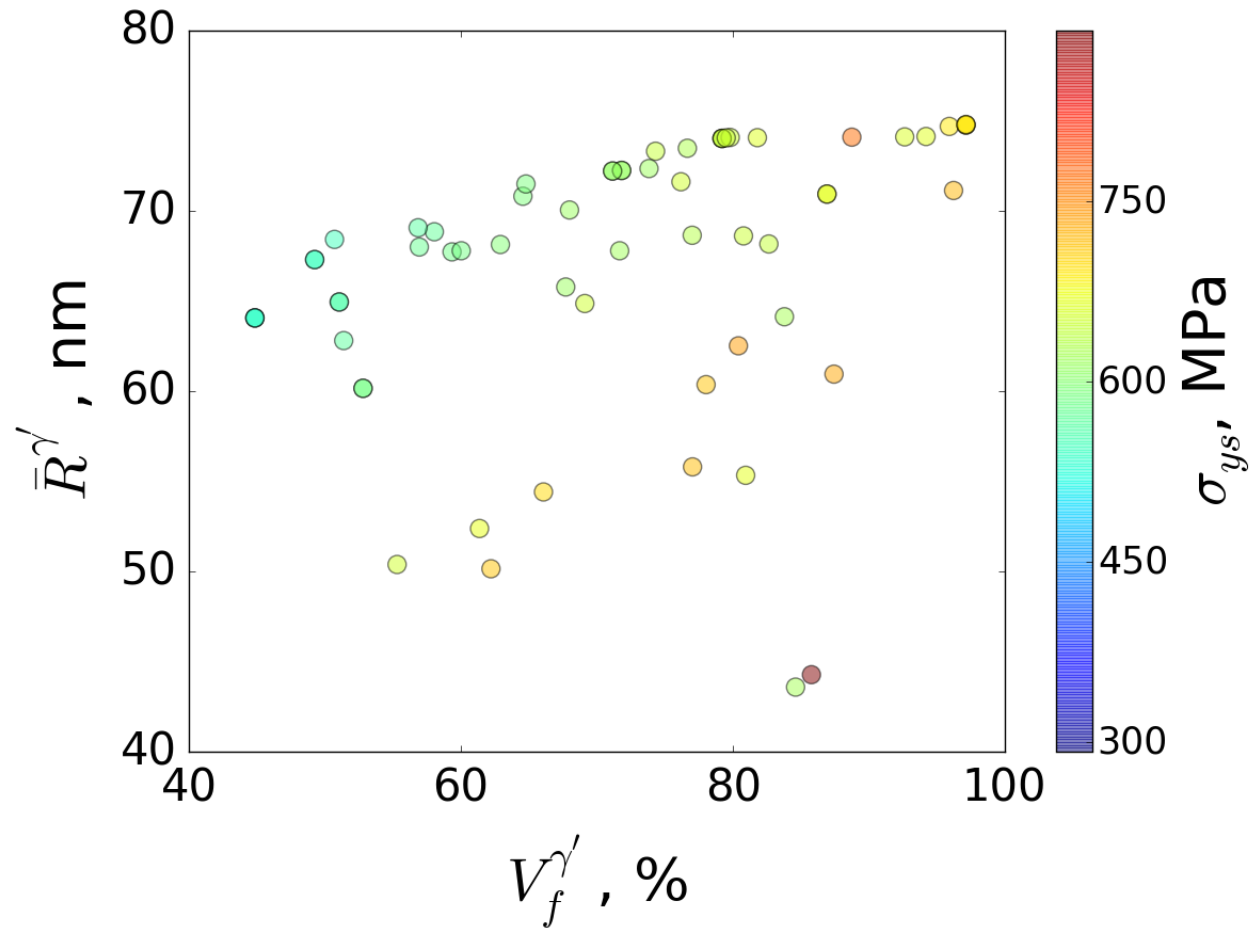
## Input conditions

	$C_{Al}, \%$	$C_{Cr}, \%$	$T_p, K$
Min	10	10	1123
Max	25	20	1473

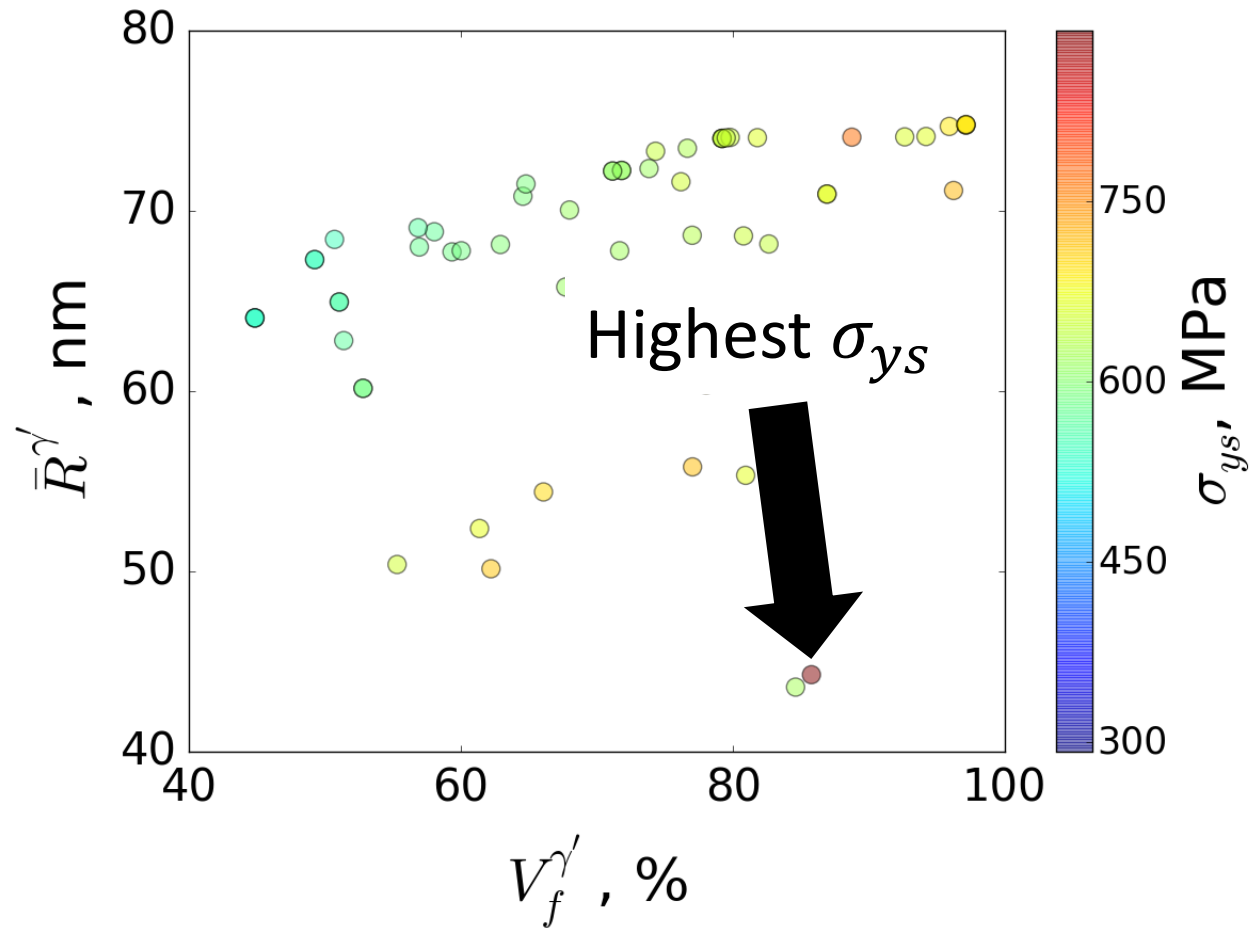
- Objective: high **work to necking** ( $E_{WNTN}$ ) at  $T_s = 1123K$
- Pass the calculations while  $\bar{v}_f^{r'} < 0.4$
- 6 bits of memory is utilized for 1 variable
- 6 samples are selected in 1 generation and 10 generations are calculated



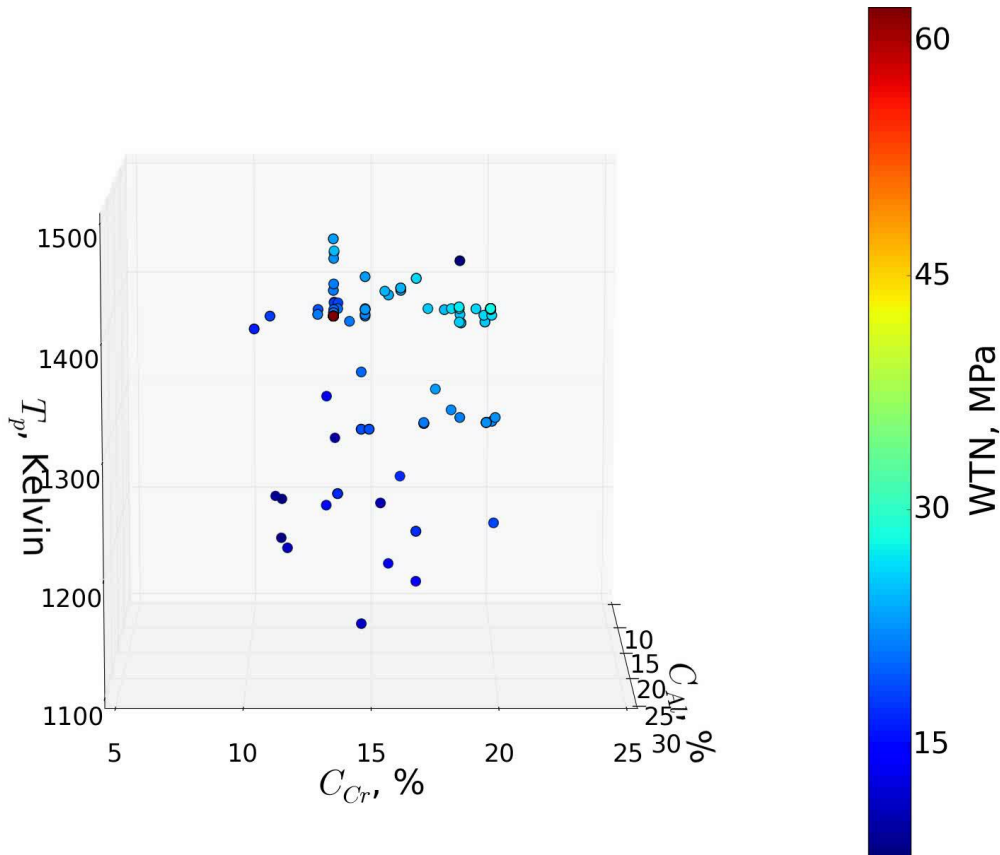
# Optimization



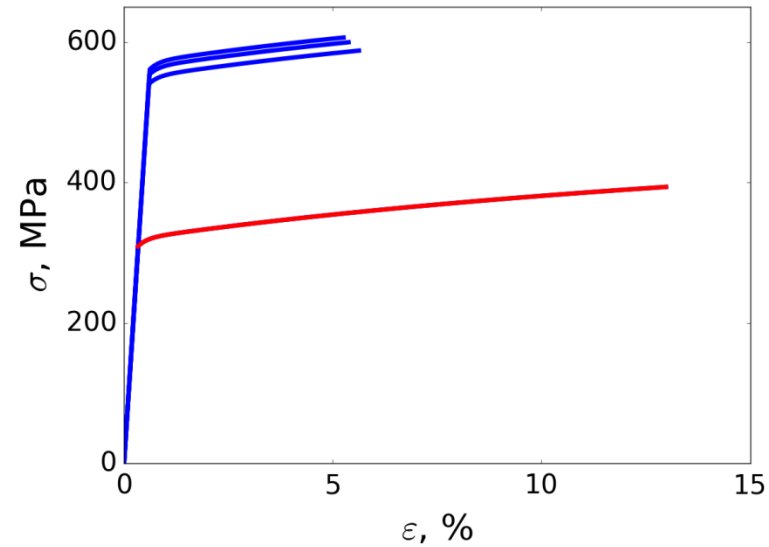
# Optimization



# Optimization - WTN



$C_{Al}, \%$	0.231
$C_{Cr}, \%$	0.195
$T_p, \text{Kelvin}$	1450
$\sigma_{UTS}, \text{MPa}$	394
$\epsilon_{UTS}, \%$	12.98



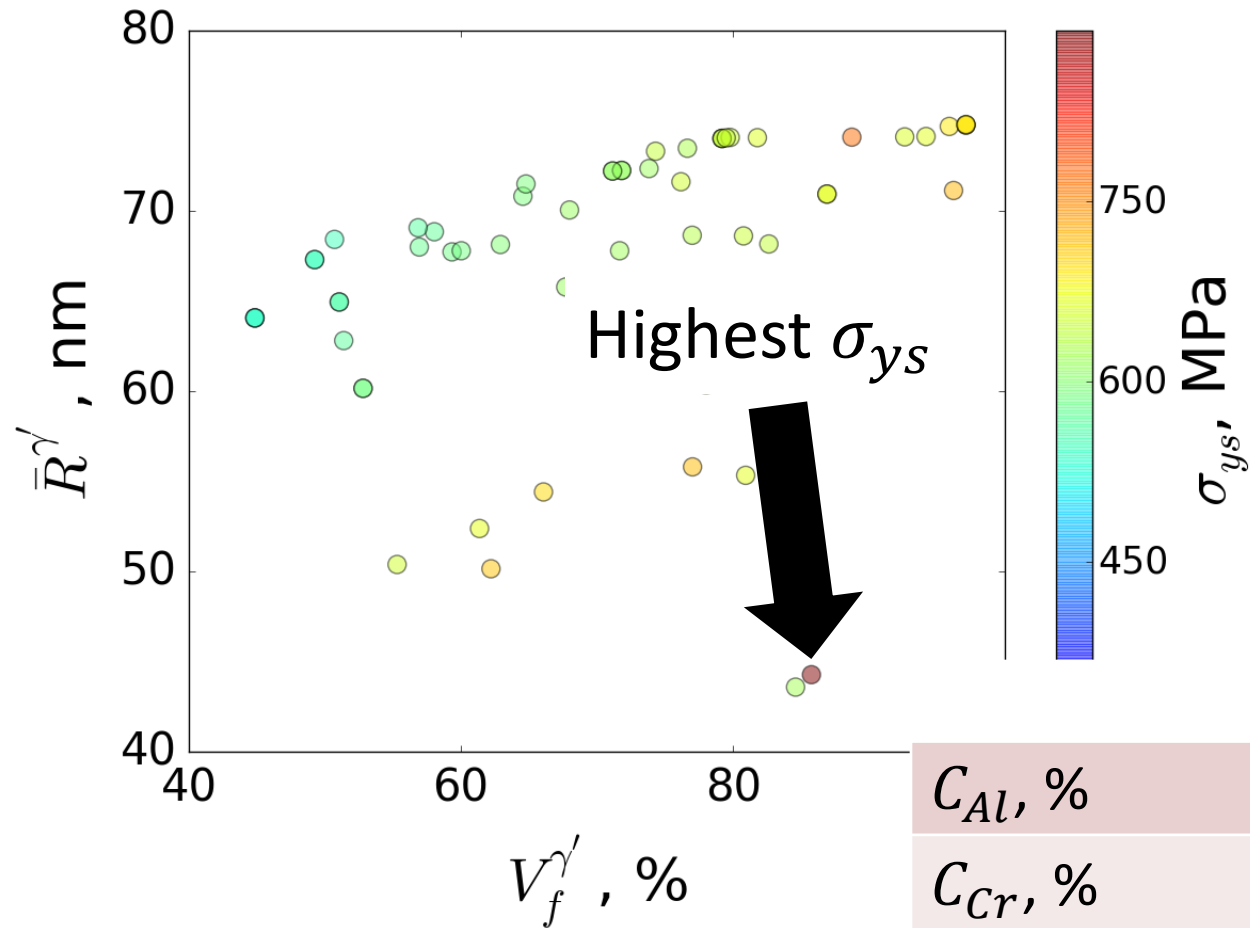
# Summary

---

- The optimization of Ni-Al-Cr ternary system is demonstrated.
- With proper  $E_{INT}$  and  $N_0$ , nucleation-growth-coarsening models successfully approach  $\gamma'$  precipitation in binary and ternary system.
- The yield stress and young's modulus are calculated by empirical formulas and PyMKS package, respectively.
- The IRT model is implemented to simulating the plastic deformation.
- To optimize the chemical composition, Genetic Algorithm is used as the close loop of process-structure-properties.



# Optimization



$C_{Al}$ , %	0.174
$C_{Cr}$ , %	0.110
$T_p$ , Kelvin	1250
$\sigma_{ys}$ , MPa	891